Published in final edited form as:
*Hear Res*. 2011 May ; 275(1-2): 66–80. doi:10.1016/j.heares.2010.12.002.

# Conditional deletion of *Atoh1* using *Pax2-Cre* results in viable mice without differentiated cochlear hair cells that have lost most of the organ of Corti

**Ning Pan**[1], **Israt Jahan**[1], **Jennifer Kersigo**[1], **Benjamin Kopecky**[1], **Peter Santi**[2], **Shane Johnson**[2], **Heather Schmitz**[2], and **Bernd Fritzsch**[1]

[1] University of Iowa, Department of Biology, Iowa City, Iowa, USA

[2] Department of Otolaryngology, University of Minnesota, Minneapolis, MN, USA

## Abstract

Atonal homolog1 (*Atoh1,* formerly *Math1*) is a crucial bHLH transcription factor for inner ear hair cell differentiation. Its absence in embryos results in complete absence of mature hair cells at birth and its misexpression can generate extra hair cells. Thus *Atoh1* may be both necessary and sufficient for hair cell differentiation in the ear. *Atoh1* null mice die at birth and have some undifferentiated cells in sensory epithelia carrying *Atoh1* markers. The fate of these undifferentiated cells in neonates is unknown due to lethality. We use *Tg*(*Pax2-Cre*) to delete floxed *Atoh1* in the inner ear. This generates viable conditional knockout (CKO) mice for studying the postnatal development of the inner ear without differentiated hair cells. Using *in situ* hybridization we find that *Tg*(*Pax2-Cre*) recombines the floxed *Atoh1* prior to detectable *Atoh1* expression. Only the posterior canal crista has *Atoh1* expressing hair cells due to incomplete recombination. Most of the organ of Corti cells are lost in CKO mice via late embryonic cell deaths. Marker genes indicate that the organ of Corti is reduced to two rows of cells wedged between flanking markers of the organ of Corti (*Fgf10* and *Bmp4*). These two rows of cells (instead of five rows of supporting cells) are positive for *Prox1* in neonates. By postnatal day 14 (P14), most of the developing organ of Corti is lost through embryonic cell deaths, with the remaining cells transformed into a flat epithelium with no distinction of any specific cell type. However, some of the remaining organ of Corti cells express Myo7a at late postnatal stages and are innervated by remaining afferent fibers. Initial growth of afferents and efferents in embryos shows no difference between control mice and *Tg*(*Pax2-Cre*)*::Atoh1* CKO mice. Most afferents and efferents are lost in the CKO mutant before birth, leaving only few basal and a more prominent apical innervation. Afferents focus their projections on patches that express the prosensory specifying gene, *Sox2*. This pattern of innervation by sensory neurons is maintained at least until P14, but fibers target the few Myo7a positive cells found in later stages.

### Keywords

hair cell differentiation; flat epithelium; organ of Corti; innervation of the ear; conditional deletion; mouse ear mutants

*Author for correspondence: Bernd Fritzsch, University of Iowa, Department of Biology, 143 BB, Iowa City, IA, 52242, Phone number: 319-353-2969, Fax number: 319-535-1029, bernd-fritzsch@uiowa.edu.

## 1. Introduction

Proneural basic Helix-Loop-Helix (bHLH) genes have been known for 30 years as mediators of sensory cell differentiation (Ghysen et al., 1979; Ghysen et al., 2000). It has been known for over ten years that loss of the bHLH genes *Atoh1* (formerly *Math1*) and *Neurog1* (formerly *Ngn1*) eliminates hair cell and neuron differentiation in the mouse ear, respectively (Bermingham et al., 1999; Ma et al., 1998). Further work showed that expression of *Atoh1* in tissue culture (Zheng et al., 2000), embryonic ears (Gubbels et al., 2008), sensory ganglia (Jahan et al., 2010a) and even adult ears (Izumikawa et al., 2005; Kawamoto et al., 2003; Praetorius et al., 2009) can generate extra hair cells, leading to the perception that *Atoh1* is both necessary and sufficient to drive hair cell differentiation in the ear (Kelley, 2006). While compelling based on this evidence, this conclusion nevertheless cannot be fully reconciled with some data.

For example, while early work showed that many hair cell precursors die in *Atoh1* null mice (Chen et al., 2002), follow up work revealed that at least some organ of Corti cells survive and continue to express *Atoh1*-lacZ at least until birth, the latest stage this null mutant could be analyzed (Fritzsch et al., 2005b). These cells have been identified already in the initial report (Bermingham et al., 1999) and have been variously referred to as ‘supporting cells’ or ‘hair cell precursors’. More perplexing is a report that indicates that hair cells can form without *Atoh1* if surrounded by *Atoh1* expressing hair cells in chimaeric mice (Du et al., 2007). It was also shown that the prosensory domain that gives rise to hair cells is delineated much earlier by other markers such as certain neurotrophins (Farinas et al., 2001), transcription factors such as *Sox2* (Kiernan et al., 2005), *Gata3* (Karis et al., 2001; Lawoko-Kerali et al., 2004) and *Eya1* (Zou et al., 2008), supporting cell markers such as *Prox1* (Bermingham-McDonogh et al., 2006; Fritzsch et al., 2010b) and several *Fgf*'s and their receptors (Hayashi et al., 2008; Pirvola et al., 2000), cyclin kinase inhibitors (Doetzlhofer et al., 2009) and members of the delta/notch signaling family (Doetzlhofer et al., 2009; Kiernan et al., 2006). In addition, *Sox2* is known to be essential for this process and its absence leads to lack of hair cell formation (Kiernan et al., 2005). Furthermore, *Prox1*, *Jag1* and *Sox2* are at least partially retained in *Atoh1* null mice (Dabdoub et al., 2008). This indicates that molecules associated with sensory precursor and supporting cell definition and differentiation can remain expressed without *Atoh1* mediated regulation of the delta/notch lateral inhibition system (Doetzlhofer et al., 2009; Kageyama et al., 2009). Together these data suggest the possibility for a more sophisticated molecular interaction of *Atoh1* during hair cell differentiation. Most importantly, if expressions of at least some of these genes are retained after hair cell loss they could be of profound translational use for future therapies aiming to reconstitute the organ of Corti. Such genes could provide the molecular means to direct differentiation only in the organ of Corti precisely to the right space of the basilar membrane.

In order to understand how long such gene expression persists in the absence of hair cell differentiation, we bred a *Tg*(*Pax2-cre*) line (Ohyama et al., 2004) with a recently available floxed *Atoh1* line (Maricich et al., 2009). In the *Tg*(*Pax2-cre*)*::Atoh1*$^{fl/f}$, we achieved near complete and early ear specific deletion of *Atoh1* as evidenced by *Atoh1 in situ* hybridization. Only some cells in the posterior canal crista, which were positive for *Atoh1* because of incomplete recombination, developed Myo7a expression and turned into histologically recognizable hair cells. There were no *Atoh1* positive cells in the cochlea at any time and we demonstrated that most cells of the organ of Corti degenerate in late embryos. Nevertheless, some remaining organ of Corti cells become Myo7a positive in particular in older postnatal mice. A ‘flat’ epithelium, instead of an organ of Corti forms that expresses *Gata3*, a transcription factor essential for normal ear and hearing development (Karis et al., 2001; Van Esch et al., 2001). The pattern of innervation of the *Atoh1*

conditional knockout mice (CKO) was comparable to the control littermate at embryonic day 14.5 (E14.5) and to *Atoh1* systemic null mice at E18.5/P0 (Fritzsch et al., 2005b), but showed interesting focal projections to spotty *Sox2*-expressing domains and Myo7a positive cells in neonates. These genetically engineered mice without differentiated hair cells can be used with *Atoh1* containing viruses to test the window of opportunity during which *Atoh1* expression can still induce the full differentiation and maintenance of hair cells out of these flat epithelia.

## 2. Material and Methods

### 2.1. Mice and genotyping

All animal procedures were approved by the University of Iowa Animal Care and Use Committee (IACUC) guidelines for the use of laboratory animals in biological research (ACURF #0804066).

We bred mice carrying the *Pax2-cre* transgene (Ohyama et al., 2004) with mice carrying floxed *Atoh1* (Maricich et al., 2009; Shroyer et al., 2007), resulting in conditional knockout mice with the genotype *Tg*(*Pax2-cre*)*::Atoh1*$^{f/f}$ at the expected Mendelian ratio. The littermates with the genotype of *Tg*(*Pax2-cre)::Atoh1*$^{f/+}$ *or Atoh1*$^{f/f}$ were used as controls. Offspring were genotyped by PCR analysis of the tail DNA using *Cre*-specific primers (forward: 5′-CCT GTT TTG CAC GTT CAC CG-3′ and reverse: 5′-ATG CTT CTG TCC GTT TGC CG-3′) which produced a 280 bp product, and *Atoh1* specific primers (forward: 5′-AGC GAT GAT GGC ACA GAA G-3′ and reverse: 5′-GAA GTC AAG TCG TTG CTA AC-3′) which produced a 300 bp product from wild-type *Atoh1* coding region and a 500 bp product from the floxed allele.

All mice were perfused with 4% paraformaldehyde (PFA) in 0.1 M phosphate buffer (pH 7.4) using a peristaltic pump following a lethal dose of Avertin anesthesia (1.25% of 2.2.2-tribromoethanol at a dose of 0.025 ml/g of body weight). Heads were isolated and fixed in 4% PFA at least for 24 hours before the ears were dissected in 0.4% PFA for further processing.

### 2.2. *In situ* hybridization

*In situ* hybridization was performed using a RNA probe labeled with digoxigenin. The plasmids containing the cDNAs were used to generate the RNA probe by *in vitro* transcription. The dissected ears were dehydrated in 100% methanol and rehydrated in a graded methanol series and then digested briefly with 20 μg/ml of Proteinase K (Ambion, Austin, TX, USA) for 15–20 minutes. Then the samples were hybridized overnight at 60°C to the riboprobe in hybridization solution containing 50% (v/v) formamide, 50% (v/v) 2X saline sodium citrate and 6% (w/v) dextran sulphate. After washing off the unbound probe, the samples were incubated overnight with an anti-digoxigenin antibody conjugated with alkaline phosphatase (Roche Diagnostics GmbH, Mannheim, Germany). After a series of washes, the samples were reacted with nitroblue phosphate/ 5-bromo, 4-chloro, 3-indolil phosphate (BM purple substrate, Roche Diagnostics GmbH, Mannheim, Germany), which is enzymatically converted to a purple colored product. The ears were mounted flat in glycerol and viewed in a Nikon Eclipse 800 microscope using differential interference contrast microscopy and images were captured with Metamorph software.

For sections, the reacted ears were embedded in resin, sectioned (see below) and imaged with a Nikon E800 microscope.

### 2.3. Lipophilic dye tracing

The heads of the mice were cut sagittally at the midline and two different colored lipophilic dye-soaked filter strips (Fritzsch et al., 2005a; Tonniges et al., 2010) were inserted approximately into the alar plate of rhombomere 2 and the basal plate of rhombomere 4 to label the afferent and efferent fibers to the inner ear, respectively. Half heads were kept in 60°C oven for about 24 hours for proper diffusion. Then the ears were dissected out for analysis and images were taken with a Leica TCS SP5 confocal microscope.

### 2.4. Immunochemistry

The ears were dehydrated in 100% ethanol and after rehydration with graded ethanol and PBS the samples were blocked with 2.5% normal goat serum in PBS containing 0.25% Triton-X-100 for 1 hour. Then the primary antibodies for activated Caspase3 (1:100; Cell Signaling, 9661), Myo7a (1:200; Proteus Biosciences, 25–6790), Prox1 (1:500; Covance, PRB-238C), Sox2 (1:200; Millipore, AB5603), and Tubulin (1:800; Sigma, T7451) were added and incubated for 48 hours at 4 C. After several washes with PBS, corresponding secondary antibodies (1:500; Alexa fluor molecular probe 647, 532, or 488; Invitrogen) were added and incubated overnight at 4°C. The PSVue480 and Hoechst dyes were then added and incubated for 15 minutes at room temperature. The ears were washed with PBS and mounted in glycerol and images were taken with a Leica TCS SP5 confocal microscope.

### 2.5. Plastic embedding and Stevenel's Blue staining

The ears were fixed in 2.5% glutaraldehyde overnight followed by several washes with 0.1 M phosphate buffer and then fixed with 1% osmium tetroxide for 1 hour. Samples were then dehydrated in graded ethanol and propylene oxide, embedded with Epon 812 in beam capsules and polymerized at 60°C for at least 24 hours. Two μm sections were cut using a Reichert Ultratome and stained at 60°C with Stevenel's Blue (del Cerro et al., 1980) made of 2% potassium permanganate and 1.3% methylene blue.

### 2.6. TSLIM

**Thin-Sheet Laser Imaging Microscopy (TSLIM)—**Fixed three week old CKO and control littermate ears were dissected from the skull. Ears were decalcified with 10% EDTA, dehydrated and cleared with Spalteholz solution (5:3 methyl salicylate:benzyl benzoate). Specimens were stained in Rhodamine B isothiocyanate (1mg/200mL in Spalteholz for one day) and imaged with TSLIM at the University of Minnesota (Santi et al., 2009). Whole inner ears were nondestructively, serially sectioned in a mid-modiolar plane at 5μm thickness. A complete *z*-stack of optical sections containing the full dimension of the inner ear resulted in 270 well-registered images using a Retiga 2000 digital camera on TSLIM. Image voxel size was 1.5×1.5×5 μm. Images were adjusted for brightness and contrast.

**3D reconstruction—**The z-stack for each inner ear was loaded into Amira ver. 5.2 (Visage Imaging, San Diego, CA) for 3D reconstruction of inner ear structures. To isolate different inner ear structures and compute their morphometric parameters a process called segmentation was used. Using Amira's semi-automated tools, the borders of each structure of interest were outlined in a different color in every section of the stack. After segmentation, Amira provided isosurface volume reconstructions of individual inner ear structures as well as an estimate of their volume based on voxel size. Structure centroids were determined by the centerline tree module in Amira. To compute the spiral length of each structure, a smooth B-spline curve fit was computed from each structure's centroid. Measurements are included in Table 1.

## 3. Results

### 3.1. *Tg*(*Pax2-Cre*) led to early and near complete loss of *Atoh1* expression

We first wanted to establish that in the CKO mice the recombination of the floxed *Atoh1* gene was complete and happened prior to *Atoh1* expression, which starts in wild-type mice around E11 in the vestibular sensory epithelia and around E13.5 in the cochlea (Matei et al., 2005). We checked the expression of *Atoh1* with *in situ* hybridization assuming that levels of *Atoh1* mRNA that cannot be detected with this technique have little to no effect on hair cell differentiation. We could not detect even traces of *Atoh1* mRNA in almost all sensory epithelia with this approach as early as E13.5 (Fig. 1B) except for limited expression in the posterior canal crista and occasionally in the anterior canal crista (Fig. 1B), likely reflecting differential regulation of the *Pax2-cre* transgene on the heterogeneous genetic background generated with the crossing of these two lines. It was previously shown that genes expressed in the posterior canal may not be properly recombined with *Pax2-cre* (Soukup et al., 2009) and our data on *Tg*(*Pax2-cre*)*::Atoh1*$^{fl/f}$ concur with this suggestion. Thus the posterior canal crista with some remaining *Atoh1* expression can serve as an internal control for the effects of the successful elimination of *Atoh1* in other epithelia.

Previous work has shown massive hair cell reduction in *Neurog1* null mice, in particular in the saccule, (Ma et al., 2000; Matei et al., 2005) possibly due to cross-regulation of *Neurog1* and *Atoh1* (Raft et al., 2007). Recent work suggested this cross-regulation may be in part be mediated by another bHLH gene *Neurod1* (Jahan et al., 2010a). Therefore we investigated the expression of *Neurog1* and *Neurod1* in *Atoh1* CKO mice using *in situ* hybridization. Our data showed expanded expression of *Neurog1* in the utricle and saccule at E13.5 and E14.5 (Fig. 1D, H) and also of *Neurod1* at E14.5 (Fig. 1F), consistent with the cross-regulation of *Neurog1* and *Neurod1* by *Atoh1*. The expanded expression of *Neurog1* and *Neurod1* (Fig. 1D, F, H) resulted in reduction of the superior vestibular ganglion and expansion of the inferior vestibular ganglion, but did not result in any obvious change of spiral neurons in the CKO ear when examined with a neuronal marker, *Nhlh2* (Fig. 1I–J′). However, this marker showed differences in expression in subpopulations of vestibular neurons indicative of a more sophisticated interaction of several bHLH genes in sensory neuron development as previously suggested (Fritzsch et al., 2010a).

We next investigated the development of afferent and efferent innervation in these conditional mice using lipophilic dye tracing (Fritzsch et al., 2010b; Jahan et al., 2010b). Consistent with our previous finding in systemic *Atoh1* null mice (Fritzsch et al, 2005), there was no apparent difference between control and mutant mice at E14.5 with respect to afferent and efferent innervation (Fig. 1K–L′).

These data support that our mouse model has no or not enough *Atoh1* mRNA detectable by *in situ* hybridization after E13.5 and that the loss of *Atoh1* is likely complete in most sensory epithelia of the ear given the comparable cross-regulation effects on *Neurog1* and *Neurod1* upregulation as seen in *Atoh1* null ear (Jahan et al., 2010a; Raft et al., 2007). The *Atoh1* CKO mouse should therefore be identical to the systemic *Atoh1* null mouse as far as development of most epithelia, including the organ of Corti, is concerned.

### 3.2. Conditional deletion of *Atoh1* resulted in near complete absence of differentiated hair cells in a near normal ear

Unlike the *Atoh1* systemic null mice, the *Atoh1* CKO neonates did not appear to have any breathing difficulty at birth. Although the mutant mice had lower body weight compared to their control littermates (data not shown), some can survive for about three weeks but died within a few days after weaning. The oldest *Atoh1* CKO mice obtained thus far were kept with the mothers past weaning age until P31. Why some mice die earlier remains unclear but

we found *Pax2-Cre* mediated upregulation of the Rosa26 marker throughout the brainstem in older neonates. This could affect functions of the pre-Botzinger complex neurons known to lead to breathing problems and perinatal deaths of *Atoh1* null mice (Rose et al., 2009). For the first time this provides us with postnatal mice to study the development of the organ of Corti without any *Atoh1* mediated hair cell differentiation for over three weeks.

In *Atoh1* CKO neonates, we confirmed that *Atoh1* was eliminated in all sensory epithelia except the posterior canal crista (Fig. 2B, B′), which had only a few hair cells as shown by Myo7a immunochemisty (Fig. 2F). The cochlea in the CKO mutant went through near normal full extension (Table 1) without differentiation of any hair cells (Fig. 2D). It was previously shown in *Atoh1* null mice that some undifferentiated cells survive and continue to express *Atoh1*-lacZ until E18.5, the latest stage these mice can be analyzed (Bermingham et al., 1999; Fritzsch et al., 2005b). Another study showed that many cells in the sensory epithelium, including supporting cells, undergo apoptosis in the *Atoh1* null mutant ear, but this was not quantified (Chen et al., 2002). To reconcile these two reports, we performed whole mount immunochemistry of activated Caspase3 to directly examine the apoptotic cells in *Atoh1* CKO ear. At E18.5, the control cochlea had very few apoptotic cells (Fig. S1A). In contrast, the *Atoh1* CKO mutant cochlea had substantially more apoptotic cells in the spiral ganglion (Fig. S1B, 2G). This suggests extensive neuronal deaths in the absence of hair cell differentiation. We also observed some apoptotic cells in the area comparable to the organ of Corti (Fig. S1B, 2H, 2H′). We further examined the cell deaths using a newly developed dye PSVue, which specifically binds to phosphatidylserine (PS) exposed on the membranes of dying cells (Krijnen et al., 2010). At E16.5, we observed a streak of PSVue positive cells in the upper middle part of the topographical organ of Corti in the mutant cochlea (Fig. 2I) but fewer in the base and none in the apex. Anti-activated Caspase3 antibody also detected dying cells with a relatively larger cell body that were rarely co-localized with PSVue (Fig. 2I′). These results are in agreement with the suggested cell death progression in which the activation of Caspase3 is followed by the loss of PS flippase and the appearance of phosphatidylserine on the cell surface. These data suggest a prolonged and extensive apoptosis of cells near the lumen as well as near the basilar membrane (Fig. 2I′), possibly indicating cell deaths of both undifferentiated hair cells and supporting cells in the organ of Corti.

Having demonstrated that *Tg*(*Pax2-cre*)*::Atoh1*$^{fl/f}$ results in complete loss of *Atoh1* expression in the cochlea at any stage, with the sole exception of some hair cells in the posterior canal crista (Fig. 2F), we could next analyze for the first time the histologic organization of the *Atoh1* mutant ear after onset of hearing in mice.

We first analyzed the histologic changes by Stevenel's Blue staining of the P14 ears. Sections through the organ of Corti of the mutant cochlea showed a single layered 'flat' epithelium on the basilar membrane (Fig. 3C, C′, E, E′, G, G′). More lateral cells showed a Hensen's and Claudius' cell like appearance (Fig. 3G, G′). These ears had a well developed spiral limbus with a tectorial membrane extending toward the undifferentiated area of the organ of Corti (Fig. 3C, E, E′, G, G′) comparable to the control littermate (Fig. 3A, A′). Sections through the vestibular sensory epithelia showed some hair cells only in the posterior canal crista (Fig. 3J′), consistent with our data on *Atoh1* and Myo7a expression (Fig. 1B, 2B, 2B′, 2F). However, other areas of the same crista and the other vestibular sensory organs were completely devoid of differentiated hair cells and an undifferentiated single cell layered epithelium was found (Fig. 3J). These data demonstrate the near normal development of the ear with topologically arranged sensory organs and acellular covering structures without formation of differentiated hair cells and supporting cells in most of the sensory organs, except for the posterior canal crista.

Spiral ganglia in Rosenthal's canal were found in *Atoh1* CKO mice only near the basal tip and in the apex (Fig. 3D, H). The middle turn had only a few neurons singly casted in bone (Fig. 3F, F′). In contrast to the adult induced neuronal cell deaths where empty spaces remain in Rosenthal's canal (Shibata et al., 2010), we found tightly fit bone space around the neurons, suggesting that little, if any cell death takes place after the initial phase of spiral neuron loss between E14.5 and P0. Close examination showed that the neurons were identical in size with no indication of Type II neurons (Fig. 3D′, F′, H′). With this exception, the overall appearance of the neurons was similar to their control littermates. Cross sections through the cochlear nerves showed massive reduction of fibers, consistent with the reduction of the neurons (Fig. 3K, K′, L, L′). To estimate the total loss of spiral neurons we counted the number of cochlear fibers as they exited the ear. We observed over 90% reduction of both the cochlea afferent and efferent fibers in the *Atoh1* CKO mutant (Table 1).

We next used Thin-Sheet Laser Imaging Microscopy (TSLIM) to analyze the overall structures of the mutant ear. Our data showed a small reduction in overall volume of the scalae (Fig. 4A–E, H, I; Table 1) and a nearly identical length of the basilar membrane (Fig. 4F, G; Table 1). However the width of the basilar membrane was reduced (Fig. 4C–G, Table 1) due to the complete absence of a recognizable organ of Corti. The basilar and the tectorial membranes had comparable volume reductions of about 50% suggesting that the shortening of the radial span of the basilar membrane and its likely effect on the biomechanics of the ear may affect postnatal growth of these essential features for non-cell based sound induced movement. The volume reduction of the Rosenthal's canal closely matched the total reduction in fibers (Fig. 4F, G; Table 1). The volume reduction in vestibular parts such as the canal cristae was also obvious with this approach (Fig. S2A–D).

### 3.3. Some innervation remained in the *Atoh1* CKO neonates

We next investigated the defects on innervation caused by the complete absence of *Atoh1* mediated hair cell differentiation. In agreement with previous work on E18.5 *Atoh1* null mice (Fritzsch et al., 2005b), Tubulin immunochemistry showed some innervation to all sensory epithelia at birth (Fig. 5B–B″, D, F). The cochlea of *Atoh1* CKO mice showed some radial fibers only in the very basal tip (Fig. 5B, B′) and a progressively increasing density of radial fibers toward the apex (Fig. 5B, B″). The upper middle turn was almost devoid of any innervation (Fig. 5B, L). Radial fibers reached what appeared to be the area of the organ of Corti but showed no terminals. Instead, fibers formed loops in most areas in proximity to the organ of Corti (Fig. 5B, L, L′), as previously described in *Atoh1* null mice (Fritzsch et al., 2005b) and reported also in mice with chemical ablation of hair cells (Shibata et al., 2010). Except for the more profound innervation to the posterior canal (Fig. 5F), there was no noticeable difference of innervation between *Atoh1* CKO and *Atoh1* null mice (Fritzsch et al., 2005b).

Previous work has shown the continued presence of Prox1 and Sox2 proteins in the apex of *Atoh1* null mice (Dabdoub et al., 2008; Fritzsch et al., 2010a). Using *in situ* hybridization we showed the presence of *Sox2* mRNA in the CKO cochlea (Fig. 5I–J′). Compared to the Sox2 protein expression in the apex of systemic *Atoh1* null mice (Dabdoub et al., 2008), *Sox2* expression in *Atoh1* CKO mice was variable (Fig. 5I, J, L) but generally extended along the entire cochlea with a patchy pattern of expression, toward the basal end of the expression (Fig. 5J, J′, L, L′). *Sox2* was also expressed in sensory neurons at this late stage and we could use this expression to effectively show the distribution of remaining sensory neurons (Fig. 5I, J).

In areas of patchy expression of Sox2 protein we found that fibers branched and ended freely (Fig. 5L, L″). Since Sox2 protein is expressed in the supporting cells in wild-type

mice at this stage (Dabdoub et al., 2008; Mak et al., 2009), we tested whether the residual expression of Sox2 correlates with the expression of *Ntf3*, a neurotrophin expressed primarily in the supporting cells of the developing cochlea (Farinas et al., 2001; Pirvola et al., 1992). While we could obtain a signal in control mouse cochlea, there was no detectable signal for *Ntf3* in *Atoh1* CKO mice (data not shown). We therefore investigated the expression of *Bdnf*, which was previously shown to be expressed in undifferentiated precursors of *Atoh1* null mice (Fritzsch et al., 2005b) and predominantly supported the apical spiral ganglia (Farinas et al., 2001). Our data showed a clear apex to base gradient of *Bdnf* expression in control mice (Fig. 5M). In the *Atoh1* CKO mice, *Bdnf* intensity was greatly reduced in the apex, sometimes not detectable with *in situ* hybridization and showed a patchy expression pattern (Fig. 5N, N′). We could detect neither *Ntf3* nor *Bdnf* in the basal tip where some innervation remained. These data suggest that some limited expression of sensory precursor/supporting cell specific genes, including *Sox2* and *Bdnf*, is possible in the absence of *Atoh1* mediated hair cell differentiation. Most importantly, this residual expression was well correlated with the remaining apical innervation of the cochlea.

We also investigated the efferent innervation using lipophilic dye tracing in P0 animals (Fig. S3A–F). Efferents grow along afferents and loss of afferents is closely followed by alterations in efferents. Compared with the control ear (Fig. S3A, A′, C, D), the *Atoh1* CKO mutant ear had greatly reduced efferents at birth (Fig. S3B, B′, E, F) as previously reported in late embryos in *Atoh1* null mice (Fritzsch et al., 2005b). We also investigated the cochlear nucleus projection of spiral afferents. However, this analysis is compromised by a neonatal appearance of *Pax2-Cre* expression in the hindbrain that eliminates *Atoh1* in cochlear nucleus neurons (data not shown). With this caveat in mind we found a reduction of afferents and the cochlea nucleus but also extensive branching of the basal turn afferents to the remaining cochlear nucleus (Fig. S3H, H′) comparable to previous data on *Ntf3* null mice that have a topographically comparable loss of spiral neurons (Fritzsch et al., 1997).

### 3.4. Loss of *Atoh1* arrested hair cell and supporting cell differentiation

We next wanted to better understand the relationship of various expressions of genes as they correlate with the apparent reduction of the organ of Corti, the residual expression of *Sox2,* the remaining innervation, and the presence of absence of differentiation of supporting cells. We first investigated the expression of *Prox1*, a marker for supporting cells, which is important in type II spiral neuron pathfinding (Bermingham-McDonogh et al., 2006; Fritzsch et al., 2010b). Like *Sox2*, *in situ* hybridization showed *Prox1* expression in patches of two rows of cells in the P0 *Atoh1* CKO cochlea instead of the five rows of supporting cells found in control (Fig. 6A, A′, C, C′). The apical tip of the CKO cochlea showed more continuous expression of *Prox1* (Fig. 6C), consistent with *Sox2* expression (Fig. 5I) implying that the reduction to two rows of *Prox1* positive cells or their complete loss is secondary to the initial upregulation. Immunochemistry for *Prox1* revealed the previously reported labeling of two pillar and three Deiter's cells in P7 control mice (Fig. 6B) but showed only very few labeled cells in the CKO mice (Fig. 6D). Pillar cells and Deiter's cells were positive for Tubulin at this stage in wild type mice but showed only an irregular and low expression in the remaining organ of Corti in CKO mice (Fig. 6B, D).

We next analyzed the relationship of *Sox2* expression to the organ of Corti in older mice. As in embryos, Sox2 expression was obvious in the greater epithelial ridge (GER) medial to the organ of Corti in both control and CKO mice (Fig. 6E–F″). In addition, the Sox2 expression overlapped with the Tubulin labeling of the supporting cells in the control organ of Corti (Fig. 6E–E″). In contrast, little Tubulin labeling and no Sox2 labeling beyond a few cells remained in CKO mice (Fig. 6F–F″). Nerve fibers ended as radial fibers near the middle of the Sox2 expression in the GER in the CKO mice (Fig. 6F′, F″). These fibers could be followed in different focal planes to the organ of Corti in the control but formed loops in the

CKO (Fig. 6F′–G′). Occasionally a few fibers extended to the area of the organ of Corti in the CKO mice (Fig. 6G′) where they formed a meshwork of fibers (Fig. 6H). The base showed projection of very limited fibers consistent with the newborn basal innervation (Fig. 6H).

We next wanted to analyze the continued decline of organ of Corti differentiation by following the supporting cells and innervation with Tubulin and the degree of differentiation using Myo7a, a hair cell marker. While nearly all of the perinatal and most of the early neonatal CKO mice showed no staining for Myo7a (Fig. 7B), we found some older mice with single cells or focal aggregates of Myo7a positive cells (Fig. 7C). These cells persisted at least until P31, the oldest stage we analyzed (Fig. 7E). These cells receive Tubulin positive radial fibers and were flanked laterally by Tubulin positive cells resembling pillar cells and phalangeal processes of Deiter's cells (Fig. 7E). This data suggest that a few cells can survive in the organ of Corti and can turn into Myo7a positive cells that receive most of the residual innervation (Fig. 7C, E). We confirmed the effective recombination of *Atoh1* in these mice with Myo7 positive organ of Corti cells by checking the complete loss of cerebellar granule cells in these mice (Fig. S4B), which depend critically on *Atoh1* for early development (Bermingham et al., 2001; Pan et al., 2009).

### 3.5 *Bmp4*, *Fgf10* and *Gata3* define the position of the organ of Corti in the absence of *Atoh1* mediated hair cell differentiation

To evaluate the development of the structures associated with the organ of Corti in the near complete absence of hair cell development, we next examined the expression of *Bmp4*, a gene expressed lateral to the organ of Corti in developing Hensen's and Claudius cells (Hwang et al., 2010; Morsli et al., 1998; Ohyama et al., 2010). A gradient of *Bmp4* expression was observed in control mice with an apex to base progression and a gradual reduction of *Bmp4* expression in most cells near the base (Fig. 8A, C). A more obvious apex to base gradient of *Bmp4* expression was detected in *Atoh1* CKO mice compared to control mice in P0 (Fig. 8B, B′) and in P7 *Bmp4* expression was limited to the apical half of the cochlea with complete loss in the base (Fig. 8D–D″). This suggests that a differentiated organ of Corti is needed to maintain *Bmp4* expression as much as Bmp4 is needed to induce differentiation of the organ of Corti (Ohyama et al., 2010).

We next investigated *Fgf10*, a gene expressed in the GER of the developing cochlea in wild-type mice (Pauley et al., 2003) partially overlapping with the expression of Sox2 in the GER (Fig. 8E, G–G″). *Fgf10* expression persisted in both P0 and P7 *Atoh1* CKO cochlea mostly in the apex with gradual reduction near the base (Fig. 8F, H–H″). The *Fgf10* expression was greatly reduced in P7 *Atoh1* CKO mice (Fig. 8H–H″), consistent with the dissolution of the GER in neonates.

We next investigated the expression of *Gata3*, a gene that causes deafness in patients with a single allele mutation (Van Esch et al., 2001) and likely acts as a proneural selector gene like its ortholog *pannier* in insects (Karis et al., 2001; Sato et al., 2000). We observed expression of *Gata3* in the approximate position of the organ of Corti in the *Atoh1* CKO mice (Fig. 8J, J′, L, L′, N). Cells in the base that expressed *Gata3* showed no indication of hair cell differentiation, but only a subset of these rather uniform epithelial cells displayed the *Gata3* expression (Fig. 8N). There was both a progressive reduction in staining intensity and a narrowing of the stained area progressing from the apex to base in the CKO mice (Fig. 8J, J′).

These data suggest that *Bmp4*, *Fgf10* and *Gata3*, which are expressed prior to *Atoh1* in ear development, are not directly regulated by *Atoh1* mediated hair cell differentiation. Apparently, absence of hair cell differentiation leads to the dedifferentiation of the organ of

Corti which in turn affects the expression levels of these genes inside and outside the organ of Corti, in particular the basal half of the cochlea.

Given that *Fgf10* and *Bmp4* flank the organ of Corti medially and laterally, we wanted to determine how the apparent loss of organ of Corti cells by cell deaths (Fig. 2H–I′) and the reduction of expression of several marker genes affected the radial dimension of the organ of Corti that is so obvious in the adult CKO ear (Fig. 4). We used a simultaneous *in situ* hybridization for both *Fgf10* and *Bmp4* to identify the organ of Corti both in whole mounts (Fig. 9A, A′, B, B′) and sections (Fig. 9A″, B″). The organ of Corti appears as an unlabeled strip of four rows of hair cells and five to six rows of supporting cells in the control cochlea (Fig. 9A–A″). In contrast, the two expression domains of *Fgf10* and *Bmp4* are much closer in the CKO mice and only one or two rows of cells intervene between them (Fig. 9B–B″). At this late developmental stage there is a change in *Fgf10* expression not noted previously (Pauley et al., 2003) as *Fgf10* appears to highlight inner hair cells (Fig. 9A′, A″). Consistent with our finding of occasional Myo7a positive cells that correspond topologically to inner hair cells (Fig. 7C, E) we found patchy aggregation of *Fgf10* in single cells corresponding in radial and vertical position to inner hair cells in the CKO mice (Fig. 9B′, B″).

In summary, we show that the ear undergoes a near normal differentiation in the absence of *Atoh1*, including convergent extension of the cochlea (Hwang et al., 2010; Kelley et al., 2009). Associated structures such as spiral limbus, spiral sulcus and tectorial membrane form almost normally with the tectorial membrane touching the mostly single-layered epithelium that has replaced the developing organ of Corti by P14 (Fig. 3). The only area of near normal differentiation of hair cells is in the posterior canal, likely related to the inability of *Tg*(*Pax2-Cre*) to fully recombine the floxed *Atoh1* as already shown for another floxed gene (Soukup et al., 2009). The pattern of innervation appears to be stable after P0, suggesting that there is limited further correction of survived neurons after the end of the neurotrophins mediated cell death phase (Fritzsch et al., 2004) that is possibly related to the few Myo7a positive cells that remain in the organ of Corti. The profound cell deaths observed in late embryos seem to result in loss of the majority of cells of the organ of Corti, approximating flanking markers to the one to two rows of organ of Corti cells that remain in neonates (Fig. 9C, D). However, a few organ of Corti cells near the GER survive, express *Fgf10* in neonates and later express Myo7a. Further studies are needed to understand the molecular basis for this survival and limited level of differentiation in the absence of Atoh1.

## 4. Discussion

### 4.1. Absence of hair cell differentiation does not affect ear morphogenesis and histogenesis

Our data on *Atoh1* CKO mice show that *Atoh1* is not necessary for most of the normal differentiation of the ear, except for the differentiation of hair cells. The near normal histological appearance of vestibular and cochlear areas including the appearance of the inner spiral sulcus and the spiral limbus indicates that the patterning processes defining these areas act independently of hair cell differentiation and may at best be dependent on the undifferentiated organ of Corti cells. This result is surprising given the ability of *Atoh1* expressing hair cells to organize *in vitro* (Woods et al., 2004) and *in vivo* (Jahan et al., 2010a) the formation of supporting cells and even ear like vesicles around them if misexpressed in the sensory ganglion. One explanation may be that *Atoh1* expressing differentiating hair cells only reinforce in normal development the epithelial organization pattern generated by other genes. These data extend previous findings on expression of several organ of Corti specific genes in *Atoh1* null mice (Dabdoub et al., 2008; Fritzsch et al., 2005b). *Atoh1* seems to act in the ear mostly as a maturation factor for hair cells but

does not act as a typical cell fate determining bHLH factor as in the cerebellum (Flora et al., 2009) and intestine epithelium (Ray et al., 2007; Shroyer et al., 2007). This conclusion is consistent with our previous work on the expression of *Atoh1*-lacZ reporter in *Atoh1* null mice (Fritzsch et al., 2005b) and the data suggesting expression of *Atoh1* only after hair cells have exited the cell cycle (Lee et al., 2006; Matei et al., 2005). In contrast, *Atoh1* is expressed in proliferating precursors in other developing systems (Flora et al., 2009; Pan et al., 2009).

Overall, our data show much less differentiation of the organ of Corti compared to previously reported *Pou4f3* mutant mice, which show initial formation of hair cells followed by late embryonic hair cell loss (Hertzano et al., 2004; Xiang et al., 2003). *Pou4f3* null mice show formation of some pillar cells, which may have had enough interaction with differentiating hair cells before hair cells die to initiate and partially complete their differentiation and maintain this differentiation for several months (Pauley et al., 2008). Interestingly, the few Myo7a positive cells that are found medial to the pillar cells in some older *Atoh1* CKO mice suggest that at least some residual but incomplete differentiation is possible without *Atoh1*. This finding is comparable to the data recently obtained in *Neurod1* null mice. In these mice most of the sensory neurons die but some appear to survive and are converted into hair cells inside the ganglia, apparently under the control of *Atoh1* (Jahan et al., 2010a). It remains to be shown which other, possibly bHLH gene(s) (Fritzsch et al., 2010a) are upregulated in postnatal mice to rescue and partially differentiate these cells in the organ of Corti to at least express Myo7a.

Our data do not directly challenge the results of chimaeric expression that suggest a regulation of hair cell differentiation of *Atoh1* null cells by nearby *Atoh1* positive hair cells (Du et al., 2007). However, if this were true we would have expected to see more histologically identifiable hair cells in the posterior canal crista than what can be identified with *Atoh1 in situ* hybridization. This is clearly not the case, arguing that at least in the vestibular sensory epithelia our data do not support the notion of induction of hair cell differentiation of *Atoh1* null cells by *Atoh1* positive cells (compare Fig. 2B′, 2F, 3J′). However, the late appearance of Myo7a positive cells in the *Atoh1* CKO cochlea could indicate that further differentiation of these cells might be possible if *Atoh1* positive cells were near them as previously suggested (Du et al., 2007). Most importantly, we have generated a mouse model that will allow testing this idea by monitoring which cells most likely respond to *Atoh1* using viral transfection (Izumikawa et al., 2005; Praetorius et al., 2010). Using GFP labeling with the vectors (Shibata et al., 2010) could also show if and how far such differentiation can spread from single transfected cells that differentiate as hair cells. Our mice can also help to reveal at which point in time the remaining cells of the flat epithelium will stop responding to *Atoh1* transfection, as is the case with the chemically induced flat epithelium (Izumikawa et al., 2008).

### 4.2. Neurons develop and project normally, then undergo rapid loss in embryos but are stable in neonates

Our previous work has shown that neurons can develop and project to the sensory epithelia in the absence of any hair cell differentiation in *Atoh1* null mice (Fritzsch et al., 2005b), indicating that hair cells *per se* do not provide an attraction beyond the expression of neurotrophins in supporting cells and hair cells. There is a rapid decline of the innervation density in *Atoh1* CKO mice between E14.5 and P0 that is overlapping with the well known phase of extensive dependency on neurotrophins (Farinas et al., 2001; Fritzsch et al., 2004). We previously showed some residual expression of the neurotrophin *Bdnf* in the apex of newborn *Atoh1* null mice correlating with the highest density of afferent innervation (Fritzsch et al., 2005b). Since we could not extent this observation into neonates due to

neonatal lethality of *Atoh1* null mice (Bermingham et al., 1999), we had to leave open whether this trend would continue leading to a rapid loss of all innervation in neonates.

Our data on *Atoh1* CKO mice confirm the rapid loss of innervation in embryos but show a surprising maintenance of the pattern of residual innervation after this initial cell death. For at least two weeks there is no apparent change in the pattern of innervation. In addition, the empty spaces found in Rosenthal's canal after neuronal deaths (Shibata et al., 2010) do not form. In *Atoh1* CKO mice, areas in the basal tip and the apex that contain neurons at P0 (Fig. 5B–B″, 5L) remain until P14 (Fig. 3D, 3H). In contrast, solid bone instead of a canal is found in the middle turn where no neurons remain at P0 (Fig. 3F, 5B, 5L).

The data show that neuronal cell deaths come to a near complete halt around birth in these mice. This is so despite the fact that the phase after P0 is characterized by the near complete demise of the embryonic organ of Corti with the formation of the spiral sulcus and a one cell layer thick 'flat' epithelium after P7 almost throughout the cochlea. These data on a genetically engineered mouse with hair cell loss agree with data in humans where only a slow loss of sensory neurons after the demise of hair cells was reported (Linthicum et al., 2009; Nadol et al., 2006; Spoendlin et al., 1990) and on data generated in another genetically engineered mouse model, the *Pou4f3* null mice that also showed surprisingly long retention of some innervation (Pauley et al., 2008). Our CKO mice can provide a valuable model to test the molecular basis of this long term sensory neuron retention in the absence of organ of Corti differentiation.

We report that there is some *Bdnf* in the undifferentiated cells that by their topology would represent 'undifferentiated hair cells' in the apex of the organ of Corti. There may also be expression of *Ntf3* detectable by q-PCR (Morris et al., 2006) but we could not detect a clear signal using *in situ* hybridization. We are currently breeding mice with a *Foxg1-Cre* line which has less overlap with the *Atoh1* expression in the brainstem (Hebert et al., 2000; Pauley et al., 2006) to generate possibly even longer surviving mice to test long term effects of loss of hair cells on viability of sensory neurons.

### 4.3. Absence of hair cell differentiation does not affect expression of markers adjacent to and within the organ of Corti

Previous work has shown that genes such as *Bdnf, Sox2, Jag1,* and *Prox1* that are expressed prior to *Atoh1* in the undifferentiated sensory precursor cells remain expressed in *Atoh1* null mice (Dabdoub et al., 2008; Fritzsch et al., 2010b; Fritzsch et al., 2005b). We confirm and extend these previous findings and show that additional genes are expressed near the developing organ of Corti of *Atoh1* CKO mice.

Previous work has shown that *Bmp4* is expressed in Hensen's and Claudius cells bordering the organ of Corti (Hwang et al., 2010; Morsli et al., 1998; Ohyama et al., 2010). Using *Bmp4 in situ* hybridization we show that this marker lateral to the organ of Corti is not affected by the absence of hair cell differentiation in its radial expression. However, there is progressive longitudinal loss of expression, paralleling the base to apex progression of differentiation. We also used an *Fgf10 in situ* hybridization, a marker for the greater epithelial ridge immediately medial to the inner hair cells (Pauley et al., 2008; Pauley et al., 2003). Our data suggest that the apical expression of this gene is retained whereas the basal turn expression is nearly or completely gone prematurely compared to its loss in wild-type mice. We followed up on the fate of this expression during the transition period of greater epithelial ridge transformation to the inner spiral sulcus in neonates. Our data show that the *Fgf10* expression disappears coincident with the loss of GER cells in the *Atoh1* CKO and wild type mice. These data suggest that flanking markers for the organ of Corti remain expressed to identify the shrinking organ of Corti.

This radial shrinkage comes about through the loss of precursor cells of the organ of Corti through late embryonic cell deaths (Fig. 2I, J). Our data suggest that this is more extensive than previous data implied (Chen et al., 2002; Fritzsch et al., 2005b) and leads to the near complete loss of all cells of the organ of Corti between the flanking markers of *Bmp4* and *Fgf10* (Fig. 9C, D). Already at birth, only two rows of organ of Corti cells (instead of five rows of supporting cells found in wild type mice) are positive for *Prox1* (Fig. 6). Surprisingly, the few remaining cells of the organ of Corti can occasionally express the hair cell marker Myo7a and show pillar cell-like expression of Tubulin (Fig. 7). Why some cells of the organ survive and are even able to differentiate in the absence of *Atoh1* requires further research.

*Gata3* is highly expressed in the developing organ of Corti (Karis et al., 2001; Lawoko-Kerali et al., 2004). Humans suffer from hearing loss when a single allele is mutated (Van Esch et al., 2001), indicating the importance of *Gata3* for cochlear sensory development. Our data show that the expression of *Gata3*, which is clearly present several days prior to expression of *Atoh1* in the ear (Karis et al., 2001; Matei et al., 2005), remains and defines the organ of Corti even in the absence of any overt cytological differentiation characterizing the organ of Corti as such. *Gata3* is thus a good candidate gene to isolate promoter elements that may be useful to drive regeneration of the organ of Corti even in the flat epithelium that remains after hair cell loss. It remains to be shown if these genes are equally expressed in other mouse models with chemically induced hair cell loss or whether the antibiotic treatment causes additional thus far undetected effects in the gene expression profiles of the supporting cells.

**In conclusion—**our data show that *Atoh1* CKO mice undergo a rapid change of the embryonic prosensory epithelium through exaggerated cell deaths that result in near complete cellular loss of the organ of Corti. Some of the few surviving cells express the hair cell marker Myo7a. The expression of certain transcription factors and overall differentiation of the ear is not affected by this near complete loss of the organ of Corti. Identifying promoter regions of the remaining transcription factors might be useful to reconstitute the organ of Corti in these mice.

### Research highlights

- *Atoh1* is needed for hair cell differentiation but null mice are not viable.
- Conditional deletion of floxed *Atoh1* (*Atoh1* CKO) leads to viable mice without differentiated cochlea hair cells.
- *Atoh1* CKO mice show rapid loss of afferents prior to birth but show no change after birth.
- Afferents project primarily to precursor cells identified by *Sox2* expression.
- The organ of Corti loses most of its hair cell and supporting cell precursors through apoptosis but occasionally some cells remain and stain positively for Myo7a and Tubulin.
- The organ of Corti is mostly replaced by a flat epithelium that expresses markers such as *Fgf10*, *Gata3* and *Bmp4*.

## Supplementary Material

Refer to Web version on PubMed Central for supplementary material.

## Acknowledgments

This work was supported by a NIH grant (R01 DC 005590) to B.F.. We express our thanks to Drs. Huda Zoghbi for providing the floxed *Atoh1* mice and Drs. T. Ohyama and A. Groves for providing the *Tg*(*Pax2-cre*) line used for this study. We wish to thank the following people for providing the plasmids used for our *in situ* hybridization experiments: Dr. Zoghbi (*Atoh1*), Dr. Tessarollo (*Bdnf*), Dr. Wu (*Bmp4*), Dr. Hogan (*Fgf10*), Dr. Engel (*Gata3*), Dr. Lee (*Neurod1*), Dr. Ma (*Neurog1*), and Dr. Cheah (*Sox2*). We also thank C. Donahue for extensive help with genotyping. The Leica TCS SP5 confocal microscope was purchased in part with a grant from the Roy. J. Carver foundation. We thank the Office of the Vice President for Research (OVPR) for support.

## References

Anniko M, Arnesen AR. Cochlear nerve topography and fiber spectrum in the pigmented mouse. Arch Otorhinolaryngol. 1988; 245:155–9. [PubMed: 3178564]

Bermingham-McDonogh O, Oesterle EC, Stone JS, Hume CR, Huynh HM, Hayashi T. Expression of Prox1 during mouse cochlear development. J Comp Neurol. 2006; 496:172–86. [PubMed: 16538679]

Bermingham NA, Hassan BA, Wang VY, Fernandez M, Banfi S, Bellen HJ, Fritzsch B, Zoghbi HY. Proprioceptor pathway development is dependent on Math1. Neuron. 2001; 30:411–22. [PubMed: 11395003]

Bermingham NA, Hassan BA, Price SD, Vollrath MA, Ben-Arie N, Eatock RA, Bellen HJ, Lysakowski A, Zoghbi HY. Math1: an essential gene for the generation of inner ear hair cells. Science. 1999; 284:1837–41. [PubMed: 10364557]

Campbell JP, Henson MM. Olivocochlear neurons in the brainstem of the mouse. Hear Res. 1988; 35:271–4. [PubMed: 3198515]

Chen P, Johnson JE, Zoghbi HY, Segil N. The role of Math1 in inner ear development: Uncoupling the establishment of the sensory primordium from hair cell fate determination. Development. 2002; 129:2495–505. [PubMed: 11973280]

Dabdoub A, Puligilla C, Jones JM, Fritzsch B, Cheah KS, Pevny LH, Kelley MW. Sox2 signaling in prosensory domain specification and subsequent hair cell differentiation in the developing cochlea. Proc Natl Acad Sci U S A. 2008; 105:18396–401. [PubMed: 19011097]

del Cerro M, Cogen J, del Cerro C. Stevenel's Blue, an excellent stain for optical microscopical study of plastic embedded tissues. Microsc Acta. 1980; 83:117–21. [PubMed: 6156384]

Doetzlhofer A, Basch ML, Ohyama T, Gessler M, Groves AK, Segil N. Hey2 regulation by FGF provides a Notch-independent mechanism for maintaining pillar cell fate in the organ of Corti. Dev Cell. 2009; 16:58–69. [PubMed: 19154718]

Du X, Jensen P, Goldowitz D, Hamre KM. Wild-type cells rescue genotypically Math1-null hair cells in the inner ears of chimeric mice. Dev Biol. 2007; 305:430–8. [PubMed: 17397818]

Farinas I, Jones KR, Tessarollo L, Vigers AJ, Huang E, Kirstein M, de Caprona DC, Coppola V, Backus C, Reichardt LF, Fritzsch B. Spatial shaping of cochlear innervation by temporally regulated neurotrophin expression. J Neurosci. 2001; 21:6170–80. [PubMed: 11487640]

Flora A, Klisch TJ, Schuster G, Zoghbi HY. Deletion of Atoh1 disrupts Sonic Hedgehog signaling in the developing cerebellum and prevents medulloblastoma. Science. 2009; 326:1424–7. [PubMed: 19965762]

Fritzsch B, Farinas I, Reichardt LF. Lack of neurotrophin 3 causes losses of both classes of spiral ganglion neurons in the cochlea in a region-specific fashion. J Neurosci. 1997; 17:6213–25. [PubMed: 9236232]

Fritzsch B, Eberl DF, Beisel KW. The role of bHLH genes in ear development and evolution: revisiting a 10-year-old hypothesis. Cell Mol Life Sci. 2010a

Fritzsch B, Tessarollo L, Coppola E, Reichardt LF. Neurotrophins in the ear: their roles in sensory neuron survival and fiber guidance. Prog Brain Res. 2004; 146:265–78. [PubMed: 14699969]

Fritzsch B, Dillard M, Lavado A, Harvey NL. Canal cristae growth and fiber extension to the outer hair cells require *Prox1* activity. PLoS One. 2010b; 5:1–12.

Fritzsch B, Muirhead KA, Feng F, Gray BD, Ohlsson-Wilhelm BM. Diffusion and imaging properties of three new lipophilic tracers, NeuroVue Maroon, NeuroVue Red and NeuroVue Green and their

use for double and triple labeling of neuronal profile. Brain Res Bull. 2005a; 66:249–58. [PubMed: 16023922]

Fritzsch B, Matei VA, Nichols DH, Bermingham N, Jones K, Beisel KW, Wang VY. Atoh1 null mice show directed afferent fiber growth to undifferentiated ear sensory epithelia followed by incomplete fiber retention. Dev Dyn. 2005b; 233:570–83. [PubMed: 15844198]

Ghysen A, Richelle J. Determination of sensory bristles and pattern formation in Drosophila. II. The achaete-scute locus. Dev Biol. 1979; 70:438–52. [PubMed: 478169]

Ghysen A, Dambly-Chaudiere C. A genetic programme for neuronal connectivity. Trends Genet. 2000; 16:221–6. [PubMed: 10782116]

Gubbels SP, Woessner DW, Mitchell JC, Ricci AJ, Brigande JV. Functional auditory hair cells produced in the mammalian cochlea by in utero gene transfer. Nature. 2008; 455:537–41. [PubMed: 18754012]

Hayashi T, Ray CA, Bermingham-McDonogh O. Fgf20 is required for sensory epithelial specification in the developing cochlea. J Neurosci. 2008; 28:5991–9. [PubMed: 18524904]

Hebert JM, McConnell SK. Targeting of cre to the Foxg1 (BF-1) locus mediates loxP recombination in the telencephalon and other developing head structures. Dev Biol. 2000; 222:296–306. [PubMed: 10837119]

Hertzano R, Montcouquiol M, Rashi-Elkeles S, Elkon R, Yucel R, Frankel WN, Rechavi G, Moroy T, Friedman TB, Kelley MW, Avraham KB. Transcription profiling of inner ears from Pou4f3(ddl/ddl) identifies Gfi1 as a target of the Pou4f3 deafness gene. Hum Mol Genet. 2004; 13:2143–53. [PubMed: 15254021]

Hwang CH, Guo D, Harris MA, Howard O, Mishina Y, Gan L, Harris SE, Wu DK. Role of bone morphogenetic proteins on cochlear hair cell formation: analyses of Noggin and Bmp2 mutant mice. Dev Dyn. 2010; 239:505–13. [PubMed: 20063299]

Izumikawa M, Batts SA, Miyazawa T, Swiderski DL, Raphael Y. Response of the flat cochlear epithelium to forced expression of Atoh1. Hear Res. 2008; 240:52–6. [PubMed: 18430530]

Izumikawa M, Minoda R, Kawamoto K, Abrashkin KA, Swiderski DL, Dolan DF, Brough DE, Raphael Y. Auditory hair cell replacement and hearing improvement by Atoh1 gene therapy in deaf mammals. Nat Med. 2005; 11:271–6. [PubMed: 15711559]

Jahan I, Pan N, Kersigo J, Fritzsch B. Neurod1 suppresses hair cell differentiation in ear ganglia and regulates hair cell subtype development in the cochlea. PLoS One. 2010a; 5:e11661. [PubMed: 20661473]

Jahan I, Kersigo J, Pan N, Fritzsch B. Neurod1 regulates survival and formation of connections in mouse ear and brain. Cell Tissue Res. 2010b; 341:95–110. [PubMed: 20512592]

Kageyama R, Ohtsuka T, Shimojo H, Imayoshi I. Dynamic regulation of Notch signaling in neural progenitor cells. Curr Opin Cell Biol. 2009; 21:733–40. [PubMed: 19783418]

Karis A, Pata I, van Doorninck JH, Grosveld F, de Zeeuw CI, de Caprona D, Fritzsch B. Transcription factor GATA-3 alters pathway selection of olivocochlear neurons and affects morphogenesis of the ear. J Comp Neurol. 2001; 429:615–30. [PubMed: 11135239]

Kawamoto K, Ishimoto S, Minoda R, Brough DE, Raphael Y. Math1 gene transfer generates new cochlear hair cells in mature guinea pigs in vivo. J Neurosci. 2003; 23:4395–400. [PubMed: 12805278]

Kelley MW. Regulation of cell fate in the sensory epithelia of the inner ear. Nat Rev Neurosci. 2006; 7:837–49. [PubMed: 17053809]

Kelley MW, Driver EC, Puligilla C. Regulation of cell fate and patterning in the developing mammalian cochlea. Curr Opin Otolaryngol Head Neck Surg. 2009; 17:381–7. [PubMed: 19623076]

Kiernan AE, Xu J, Gridley T. The Notch ligand JAG1 is required for sensory progenitor development in the mammalian inner ear. PLoS Genet. 2006; 2:e4. [PubMed: 16410827]

Kiernan AE, Pelling AL, Leung KK, Tang AS, Bell DM, Tease C, Lovell-Badge R, Steel KP, Cheah KS. Sox2 is required for sensory organ development in the mammalian inner ear. Nature. 2005; 434:1031–5. [PubMed: 15846349]

Krijnen PA, Sipkens JA, Molling JW, Rauwerda JA, Stehouwer CD, Muller A, Paulus WJ, van Nieuw Amerongen GP, Hack CE, Verhoeven AJ, van Hinsbergh VW, Niessen HW. Inhibition of Rho-

ROCK signaling induces apoptotic and non-apoptotic PS exposure in cardiomyocytes via inhibition of flippase. J Mol Cell Cardiol. 2010; 49:781–90. [PubMed: 20691698]

Lawoko-Kerali G, Rivolta MN, Lawlor P, Cacciabue-Rivolta DI, Langton-Hewer C, van Doorninck JH, Holley MC. GATA3 and NeuroD distinguish auditory and vestibular neurons during development of the mammalian inner ear. Mech Dev. 2004; 121:287–99. [PubMed: 15003631]

Lee YS, Liu F, Segil N. A morphogenetic wave of p27Kip1 transcription directs cell cycle exit during organ of Corti development. Development. 2006; 133:2817–26. [PubMed: 16790479]

Linthicum FH Jr, Fayad JN. Spiral ganglion cell loss is unrelated to segmental cochlear sensory system degeneration in humans. Otol Neurotol. 2009; 30:418–422. [PubMed: 19326501]

Ma Q, Anderson DJ, Fritzsch B. Neurogenin 1 null mutant ears develop fewer, morphologically normal hair cells in smaller sensory epithelia devoid of innervation. J Assoc Res Otolaryngol. 2000; 1:129–43. [PubMed: 11545141]

Ma Q, Chen Z, del Barco Barrantes I, de la Pompa JL, Anderson DJ. neurogenin1 is essential for the determination of neuronal precursors for proximal cranial sensory ganglia. Neuron. 1998; 20:469–82. [PubMed: 9539122]

Mak AC, Szeto IY, Fritzsch B, Cheah KS. Differential and overlapping expression pattern of SOX2 and SOX9 in inner ear development. Gene Expr Patterns. 2009; 9:444–53. [PubMed: 19427409]

Maricich SM, Xia A, Mathes EL, Wang VY, Oghalai JS, Fritzsch B, Zoghbi HY. Atoh1-lineal neurons are required for hearing and for the survival of neurons in the spiral ganglion and brainstem accessory auditory nuclei. J Neurosci. 2009; 29:11123–33. [PubMed: 19741118]

Matei V, Pauley S, Kaing S, Rowitch D, Beisel KW, Morris K, Feng F, Jones K, Lee J, Fritzsch B. Smaller inner ear sensory epithelia in Neurog 1 null mice are related to earlier hair cell cycle exit. Dev Dyn. 2005; 234:633–50. [PubMed: 16145671]

Morris JK, Maklad A, Hansen LA, Feng F, Sorensen C, Lee KF, Macklin WB, Fritzsch B. A disorganized innervation of the inner ear persists in the absence of ErbB2. Brain Res. 2006; 1091:186–99. [PubMed: 16630588]

Morsli H, Choo D, Ryan A, Johnson R, Wu DK. Development of the mouse inner ear and origin of its sensory organs. J Neurosci. 1998; 18:3327–35. [PubMed: 9547240]

Nadol JB Jr, Eddington DK. Histopathology of the inner ear relevant to cochlear implantation. Adv Otorhinolaryngol. 2006; 64:31–49. [PubMed: 16891835]

Ohyama T, Groves AK. Generation of Pax2-Cre mice by modification of a Pax2 bacterial artificial chromosome. Genesis. 2004; 38:195–9. [PubMed: 15083520]

Ohyama T, Basch ML, Mishina Y, Lyons KM, Segil N, Groves AK. BMP Signaling Is Necessary for Patterning the Sensory and Nonsensory Regions of the Developing Mammalian Cochlea. J Neurosci. 2010; 30:15044–15051. [PubMed: 21068310]

Pan N, Jahan I, Lee JE, Fritzsch B. Defects in the cerebella of conditional Neurod1 null mice correlate with effective Tg(Atoh1-cre) recombination and granule cell requirements for Neurod1 for differentiation. Cell Tissue Res. 2009; 337:407–28. [PubMed: 19609565]

Pauley S, Lai E, Fritzsch B. Foxg1 is required for morphogenesis and histogenesis of the mammalian inner ear. Dev Dyn. 2006; 235:2470–82. [PubMed: 16691564]

Pauley S, Kopecky B, Beisel K, Soukup G, Fritzsch B. Stem cells and molecular strategies to restore hearing. Panminerva Med. 2008; 50:41–53. [PubMed: 18427387]

Pauley S, Wright TJ, Pirvola U, Ornitz D, Beisel K, Fritzsch B. Expression and function of FGF10 in mammalian inner ear development. Dev Dyn. 2003; 227:203–15. [PubMed: 12761848]

Pirvola U, Ylikoski J, Palgi J, Lehtonen E, Arumae U, Saarma M. Brain-derived neurotrophic factor and neurotrophin 3 mRNAs in the peripheral target fields of developing inner ear ganglia. Proc Natl Acad Sci U S A. 1992; 89:9915–9. [PubMed: 1409719]

Pirvola U, Spencer-Dene B, Xing-Qun L, Kettunen P, Thesleff I, Fritzsch B, Dickson C, Ylikoski J. FGF/FGFR-2(IIIb) signaling is essential for inner ear morphogenesis. J Neurosci. 2000; 20:6125–34. [PubMed: 10934262]

Praetorius M, Hsu C, Baker K, Brough DE, Plinkert P, Staecker H. Adenovector-mediated hair cell regeneration is affected by promoter type. Acta Otolaryngol. 2009:1–8. [PubMed: 19479459]

Praetorius M, Hsu C, Baker K, Brough DE, Plinkert P, Staecker H. Adenovector-mediated hair cell regeneration is affected by promoter type. Acta Otolaryngol. 2010; 130:215–22. [PubMed: 20095092]

Raft S, Koundakjian EJ, Quinones H, Jayasena CS, Goodrich LV, Johnson JE, Segil N, Groves AK. Cross-regulation of Ngn1 and Math1 coordinates the production of neurons and sensory hair cells during inner ear development. Development. 2007; 134:4405–15. [PubMed: 18039969]

Ray SK, Leiter AB. The basic helix-loop-helix transcription factor NeuroD1 facilitates interaction of Sp1 with the secretin gene enhancer. Mol Cell Biol. 2007; 27:7839–47. [PubMed: 17875929]

Rose MF, Ren J, Ahmad KA, Chao HT, Klisch TJ, Flora A, Greer JJ, Zoghbi HY. Math1 is essential for the development of hindbrain neurons critical for perinatal breathing. Neuron. 2009; 64:341–54. [PubMed: 19914183]

Santi PA, Johnson SB, Hillenbrand M, GrandPre PZ, Glass TJ, Leger JR. Thin-sheet laser imaging microscopy for optical sectioning of thick tissues. Biotechniques. 2009; 46:287–94. [PubMed: 19450235]

Sato M, Saigo K. Involvement of pannier and u-shaped in regulation of decapentaplegic-dependent wingless expression in developing Drosophila notum. Mech Dev. 2000; 93:127–38. [PubMed: 10781946]

Shibata SB, Cortez SR, Beyer LA, Wiler JA, Di Polo A, Pfingst BE, Raphael Y. Transgenic BDNF induces nerve fiber regrowth into the auditory epithelium in deaf cochleae. Exp Neurol. 2010; 223:464–72. [PubMed: 20109446]

Shroyer NF, Helmrath MA, Wang VY, Antalffy B, Henning SJ, Zoghbi HY. Intestine-specific ablation of mouse atonal homolog 1 (Math1) reveals a role in cellular homeostasis. Gastroenterology. 2007; 132:2478–88. [PubMed: 17570220]

Soukup GA, Fritzsch B, Pierce ML, Weston MD, Jahan I, McManus MT, Harfe BD. Residual microRNA expression dictates the extent of inner ear development in conditional Dicer knockout mice. Dev Biol. 2009; 328:328–41. [PubMed: 19389351]

Spoendlin H, Schrott A. Quantitative evaluation of the human cochlear nerve. Acta Otolaryngol Suppl. 1990; 470:61–9. discussion 69–70. [PubMed: 2239235]

Tonniges J, Hansen M, Duncan J, Bassett MJ, Fritzsch B, Gray BD, Easwaran A, Nichols MG. Photo- and bio-physical characterization of novel violet and near-infrared lipophilic fluorophores for neuronal tracing. J Microsc. 2010; 239:117–34. [PubMed: 20629917]

Van Esch H, Devriendt K. Transcription factor GATA3 and the human HDR syndrome. Cell Mol Life Sci. 2001; 58:1296–300. [PubMed: 11577985]

Woods C, Montcouquiol M, Kelley MW. Math1 regulates development of the sensory epithelium in the mammalian cochlea. Nat Neurosci. 2004; 7:1310–8. [PubMed: 15543141]

Xiang M, Maklad A, Pirvola U, Fritzsch B. Brn3c null mutant mice show long-term, incomplete retention of some afferent inner ear innervation. BMC Neurosci. 2003; 4:2. [PubMed: 12585968]

Zheng JL, Gao WQ. Overexpression of Math1 induces robust production of extra hair cells in postnatal rat inner ears. Nat Neurosci. 2000; 3:580–6. [PubMed: 10816314]

Zou D, Erickson C, Kim EH, Jin D, Fritzsch B, Xu PX. Eya1 gene dosage critically affects the development of sensory epithelia in the mammalian inner ear. Hum Mol Genet. 2008; 17:3340–56. [PubMed: 18678597]

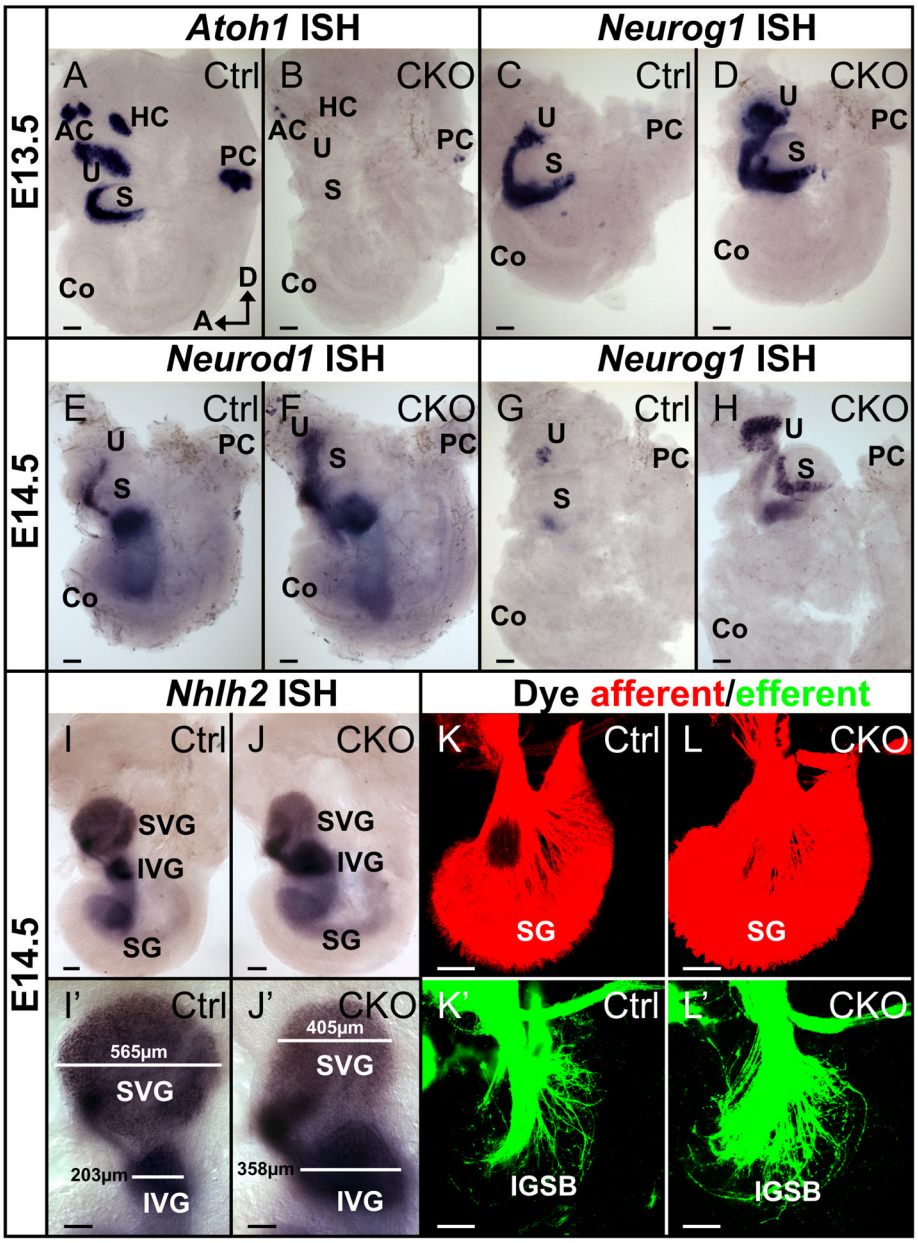


**Figure 1. Conditional deletion of *Atoh1* is early, almost complete, and affects other bHLH genes but not early neuronal development**

(**A, B**) The *Pax2-Cre* mediated recombination of floxed *Atoh1* leads to reduction and loss of *Atoh1* expression as shown by *in situ* hybridization. In E13.5 control mice, *Atoh1* is expressed in all five vestibular endorgans with limited expression in the cochlea (A). In *Atoh1* CKO mice, only some weak expression persists in the posterior crista and the anterior crista at this stage (B). (**C**–**H**)Absence of *Atoh1* leads to expression changes in other bHLH genes. At E13.5 *Neurog1* shows a wider expression in the utricle and saccule of *Atoh1* CKO mice (D) compared to their control littermates (C). At E14.5, while *Neurog1* is drastically downregulated in the control mice (G), it continues to be expressed in the CKO mice (H). An expanded expression is also seen for *Neurod1* in the mutant ear at E14.5 (E, F). (**I**–**J**′) *Nhlh2*, a neuronal marker shows near normal expression in developing ganglia in CKO mutants. However, the sizes of vestibular ganglia are obviously different: the superior

vestibular ganglion is reduced but the inferior vestibular ganglion is enlarged in CKO mutants compared to control littermates (compare the bars in I′ and J′). (**K–L′**) Lipophilic dye tracing shows that both the afferent and the efferent innervation in the *Atoh1* CKO mice (L, L′) is indistinguishable from the control littermate (K, K′). AC, anterior canal crista; Co, cochlea; HC, horizontal canal crista; IGSB, intraganglionic spiral bundle; IVG, inferior vestibular ganglion; PC, posterior canal crista; S, saccule; SG, spiral ganglion; SVG, superior vestibular ganglion; U, utricle. Bar indicates 100 μm.

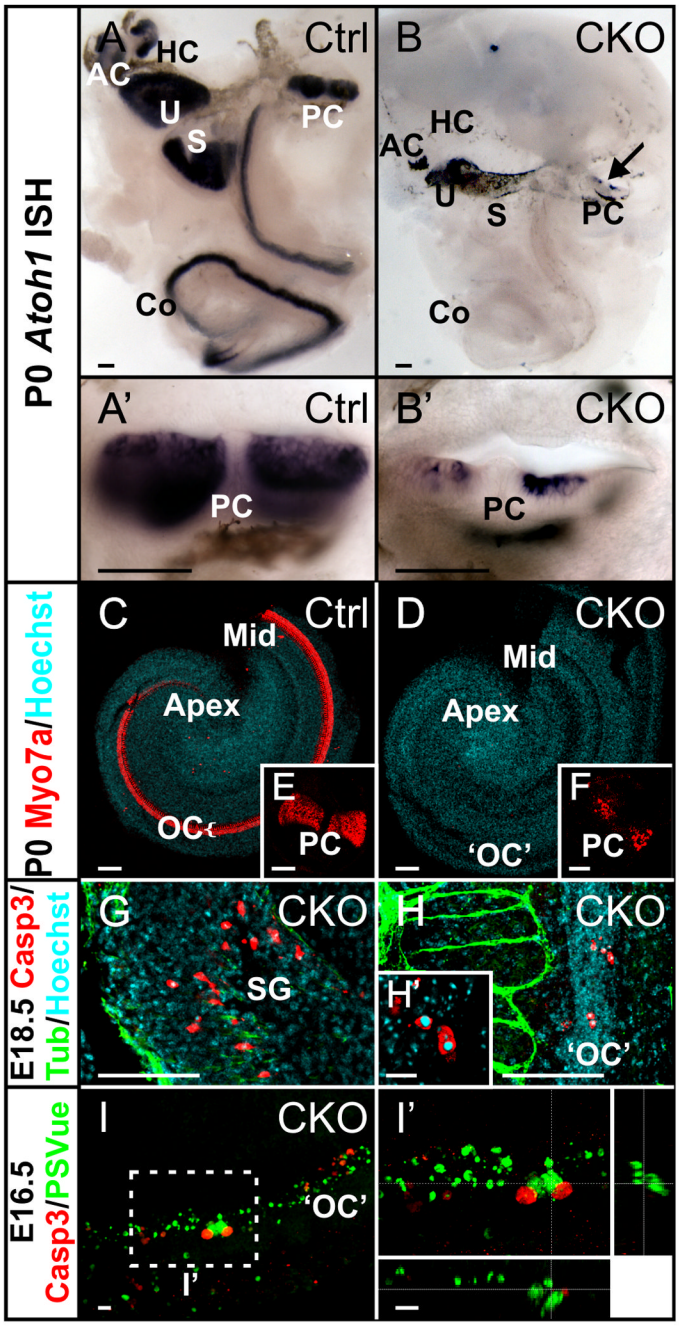


**Figure 2. Loss of *Atoh1* causes failure of hair cell differentiation and cell deaths of organ of Corti precursors and neurons**

(**A**–**B**′) *Atoh1 in situ* hybridization at P0 confirms the deletion of *Atoh1* in almost all the hair cells of the mutant ear. The control ear has strong *Atoh1* signals in all sensory epithelia (A, A′). In the CKO mutant, there is only some residual expression in the posterior canal crista (arrows in B and B′). The black patches in anterior canal crista, posterior canal crista, utricle and saccule are the pigments but not *Atoh1* signal, which shows dark purple color. (**C**–**F**) Myo7a immunochemistry shows complete loss of hair cells in the mutant cochlea. Consistent with the remaining *Atoh1* expression, a few Myo7a positive hair cells are present in the posterior canal crista (F). (**G**–**I**′) Absence of *Atoh1* causes cell deaths of neurons and

cells in the organ of Corti. In E18.5 mutant, activated Caspase3 positive cells are seen in spiral ganglion (G) and the region topographically equivalent to the organ of Corti (H). Degeneration of these cells is further evidenced by Hoechst staining of the pyknotic nuclei (H′). In E16.5 mutant, we find a streak of cells in the organ of Corti that are labeled by PSVue, which stains phosphatidylserine exposed on the cell membranes after the onset of apoptotic cell deaths (I). In I′, z-stack confocal image is optically cross sectioned through the organ of Corti (indicated by the dotted lines) and the lateral views shown on the bottom and the side reveal that PSVue positive cells are located in two cell layers, one near the lumen and one near the basilar membrane suggesting that both presumptive hair cells and supporting cells undergo cell deaths. AC, anterior canal crista; Co, cochlea; HC, horizontal canal crista; Mid, the middle part of the cochlea; OC, organ of Corti; 'OC', putative organ of Corti in *Atoh1* CKO; PC, posterior canal crista; S, saccule; SG, spiral ganglion; U, utricle. Bar indicates 100 μm except in H′-I′, where it indicates 10 μm.

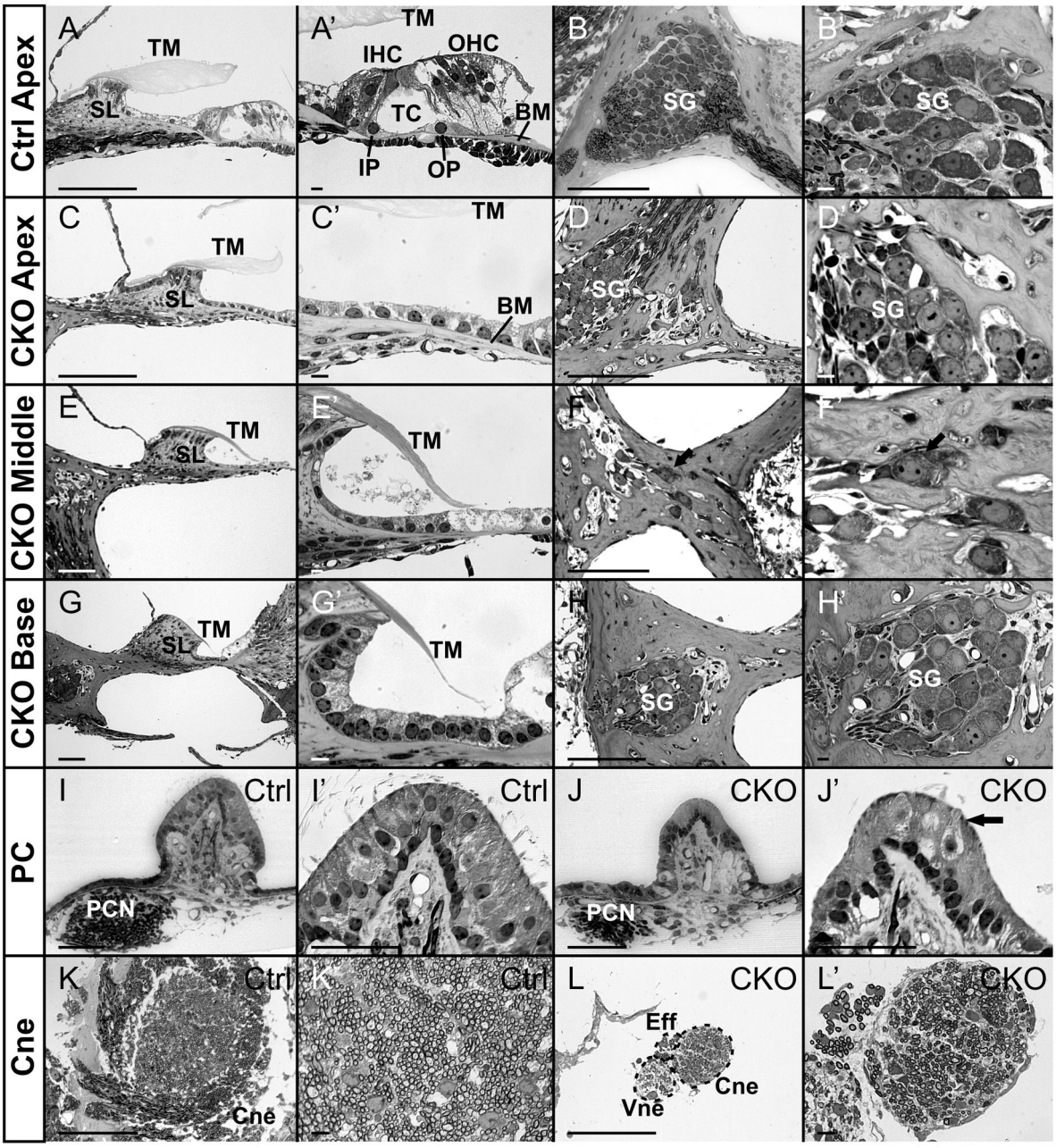


**Figure 3. Conditional deletion of *Atoh1* generates a flat epithelium and shows long-term retention of some spiral neurons in neonates**

(**A**–**H**′) Thin plastic sections through cochlea show histological changes of P14 CKO ear. The control mice form the spiral limbus and sulcus, the tectorial membrane and the organ of Corti on the basilar membrane (A, A′). Sections through the apex of the mutant cochlear reveal a flat epithelium consisting of a single row of cuboidal cells on the basilar membrane (C, C′). While the basilar membrane is progressively shorter toward the base, there is no alteration in the flat epithelium that indicates the position of the organ of Corti through the approximation of the tectorial membrane (E, E′, G, G′). Control mice have a large Rosenthal's canal filled with sensory neurons (B, B′). In CKO mice the apex and the basal tip have clusters of sensory neurons (D, D′, H, H′), whereas the middle turn has just a bony

matrix or a few isolated neurons surrounded by bone (arrows in F and F′). Note that all bone spaces are filled with neurons in both control and *Atoh1* CKO mutants, suggesting that the neuronal cell death phase is not continuing in neonates despite the transformation of the primordial organ of Corti into a flat epithelium in the absence of *Atoh1*. (**I–J′**) Some hair cells are only found in the posterior canal crista in the mutant ear. Sections through the posterior canal crista of control mice show the large bundle of the posterior canal crista nerve approaching an organ filled with many hair cells that extend apical bundles into the cupula (I, I′). The nerve approaching the posterior canal crista of *Atoh1* CKO mice are much smaller and some areas of the crista show no hair cells (J, J′, arrow indicates a differentiated hair cell). (**K–L′**) Sections through the cochlear nerve show obvious reduction of the number of nerve fibers in the CKO mutant in comparison to control (See Table 1). BM, basilar membrane; Cne, cochlear nerve; Eff, efferent nerve fibers; IHC, inner hair cell; IP, inner pillar cell; OHC, outer hair cell; OP, outer pillar cell; PC, posterior canal crista; PCN, posterior canal crista nerve; SG, spiral ganglion; SL, spiral limbus; TC, tunnel of Corti; TM, tectorial membrane; Vne, vestibular nerve. Bar indicates 100 μm in all except in A′, B′, C′, D′, E′, F′, G′, H′, K′ and L′, where it indicates 10 μm.

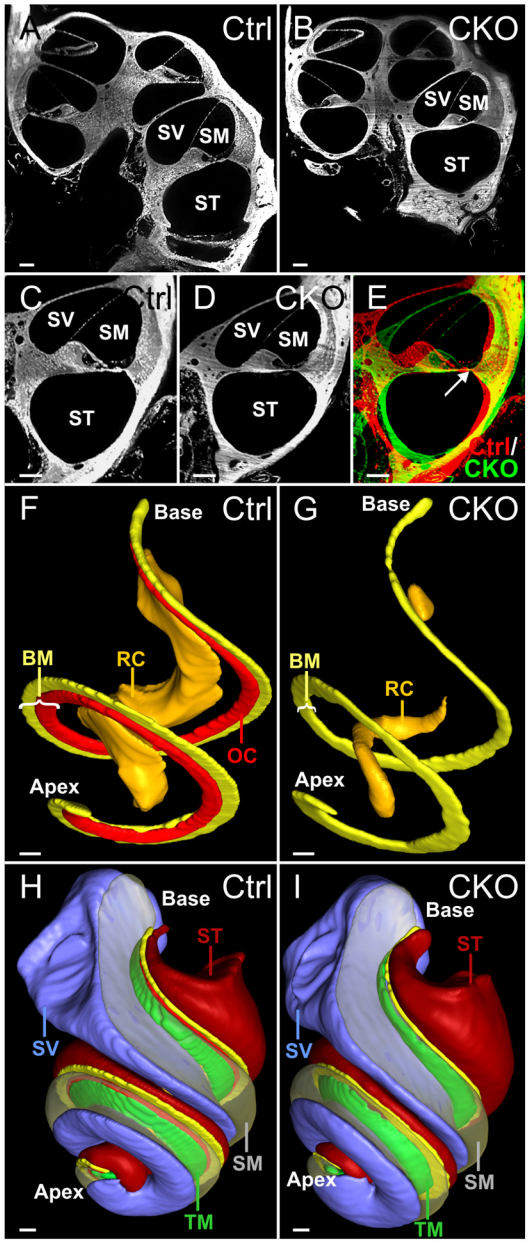


**Figure 4. TSLIM reveals comparable cochlear development with near identical length of the cochlea in CKO mutant**

(**A–E**) TSLIM 5 μm optical sections through the cochlea at comparable positions of P21 control and CKO mice show some reduction of the scalae and apparent radial reduction of basilar membrane. The narrowing of the mutant basilar membrane in the mutant ear is evident when the sections are aligned at the lateral end of the basilar membrane (arrow in E). (**F–I**) 3D reconstructions show that the overall structure of the CKO mutant cochlea is near normal despite the absence of an identifiable differentiated organ of Corti (bright red). The position of remaining Rosenthal's canal (orange) in the mutant is consistent with the topology of neurons found in plastic sections shown in Fig. 3D′, F′, H′ (G). However, the volume reduction of scalae (scala media is made transparent, scala tympani in dark red and scala vestibule in light purple) , basilar membrane (yellow) and tectorial membrane (green) do not affect the longitudinal extension of the mutant cochlea (G, I). BM, basilar membrane;

OC, organ of Corti; RC, Rosenthal's canal; SM, scala media; ST, scala tympani; SV, scala vestibule; TM, tectorial membrane. Bar indicates 100 μm.

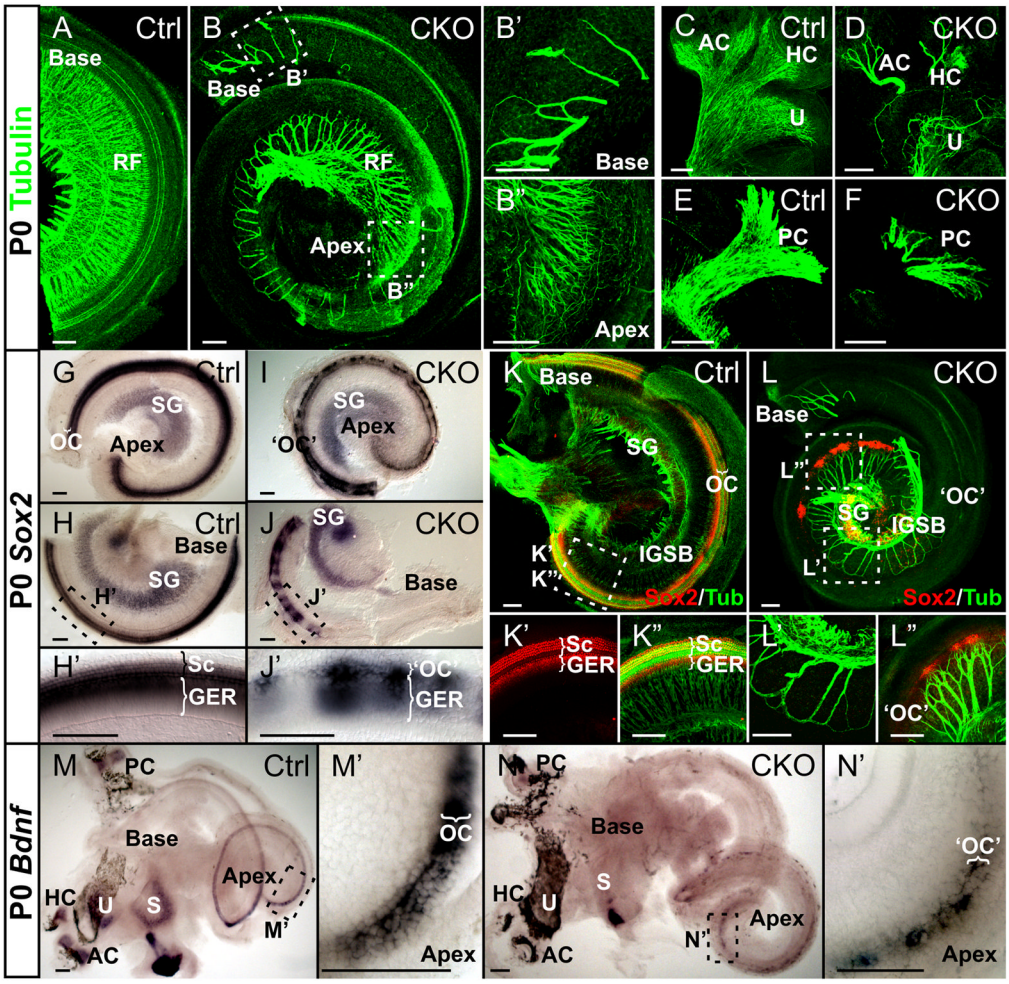


**Figure 5. The pattern of residual innervation correlates with the distribution of *Sox2* and *Bdnf* in *Atoh1* CKO mice**

(**A–F**) Immunolabeling with Tubulin shows the reduction of innervation in P0 *Atoh1* CKO mice. Radial fibers are closely spaced in the cochlea of control mice (A). In contrast, the base of the *Atoh1* CKO cochlea is almost free of any fibers (B) except for the basal tip (B′), whereas the apex (B″) and lower middle turn show some innervation with higher spacing density of radial fibers toward the apex (B, B″). The fibers in the middle turn demonstrate abnormal loop formation near the greater epithelial ridge (B). The vestibular innervation is present in all sensory epithelia but greatly reduced (D, F) in comparison to control littermate (C, E). (**G–L″**) Expression of *Sox2* persists but is reduced in mutant cochlea. *Sox2 in situ* hybridization reveals a discontinuous or patchy distribution throughout the mutant cochlea (I, J, J′). Combining Tubulin with Sox2 immunochemistry reveals Sox2 labeling in supporting cells and prosensory cells with dense innervation in control animals (K–K″). In some CKO mutants Sox2 protein is more restricted and patchy in the apex (L). Nerve fibers are attracted to those patches and branch and end freely (L″). (**M–N′**) *Bdnf* expression is greatly reduced in the *Atoh1* CKO cochlea. *In situ* hybridization shows an apex to base gradient of *Bdnf* expression in the newborn control mice (M, M′), whereas in the mutant ear, *Bdnf* expression is patchy in the apical half and is lost in the base (N, N′). AC, anterior canal crista; GER, greater epithelial ridge; HC, horizontal canal crista; IGSB, intraganglionic spiral bundle; OC, organ of Corti; ‘OC’, putative organ of Corti in *Atoh1*

CKO; PC, posterior canal crista; RF, radial fibers; S, saccule; Sc, supporting cells; SG, spiral ganglion; U, utricle. Bar indicates 100 μm.

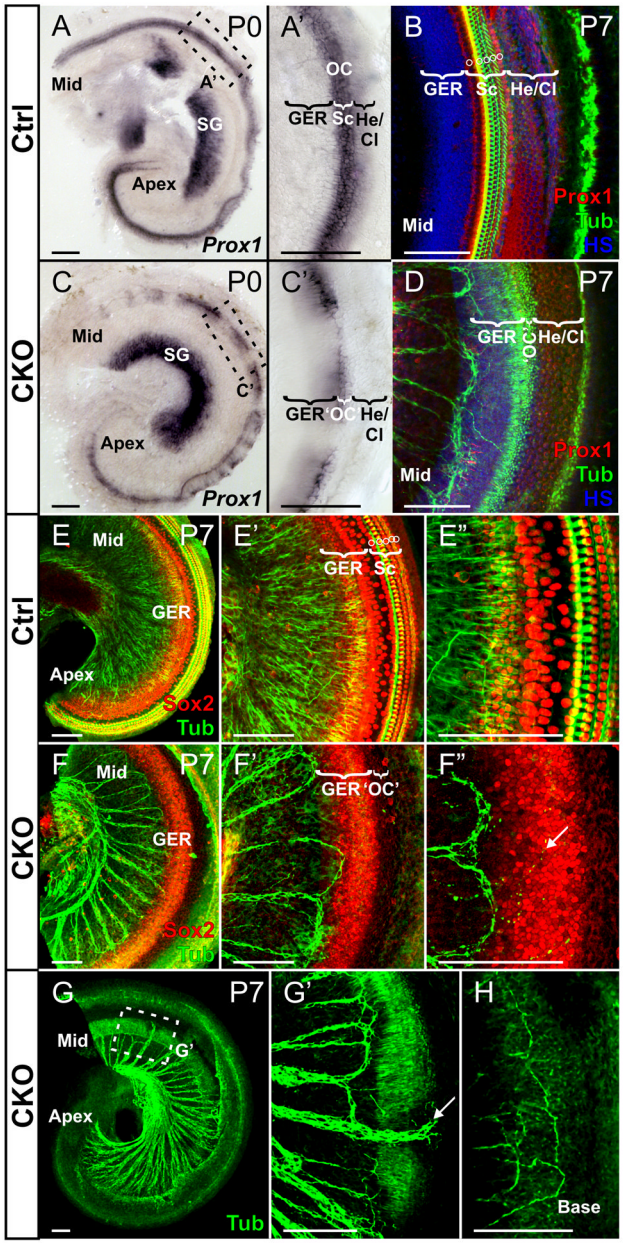


**Figure 6. Loss of *Atoh1* causes failure of organ of Corti supporting cell differentiation**

(**A–D**) Expression of Prox1 is decreased in the mutant cochlea. *In situ* hybridization shows expression of *Prox1* in the supporting cells in P0 control mice (A, A′). It is restricted to only two rows of patchy undifferentiated cells in the CKO cochlea with very weak expression in others (C, C′). In later stages (P7), immunochemistry with both anti-Prox1 and anti-Tubulin antibodies shows five rows of supporting cells labeled in the control cochlea (circles in B). In the CKO mutant littermate, there are no supporting cells detected by these markers in the unspecified organ of Corti (D). However, the topology of the organ of Corti seems to be retained and indicated by an above background expression of Tubulin (D). Nerve fibers show reduction of radial growth possibly due to the absence of differentiated organ of Corti (D). (**E–H**) Sox2 immunochemistry also shows no labeling of supporting cells in the P7 CKO cochlea. Sox2 is expressed in both supporting cells (circles in E′) and cells in greater

epithelial ridge (GER) in control cochlear, while in the CKO mutant, only the cells in GER are labeled with Sox2 (F–F″). The pattern of innervation in P7 CKO mutants forms loops before reaching the GER with occasional overshooting branches (arrows in F″ and G′) near middle turn. The base has even fewer nerve fibers (H). Cl, Claudius cells; GER, greater epithelial ridge; He, Hensen's cells; Mid, the middle part of the cochlea; OC, organ of Corti; 'OC', putative organ of Corti in *Atoh1* CKO; Sc, supporting cells; SG, spiral ganglion. Bar indicates 100 μm.

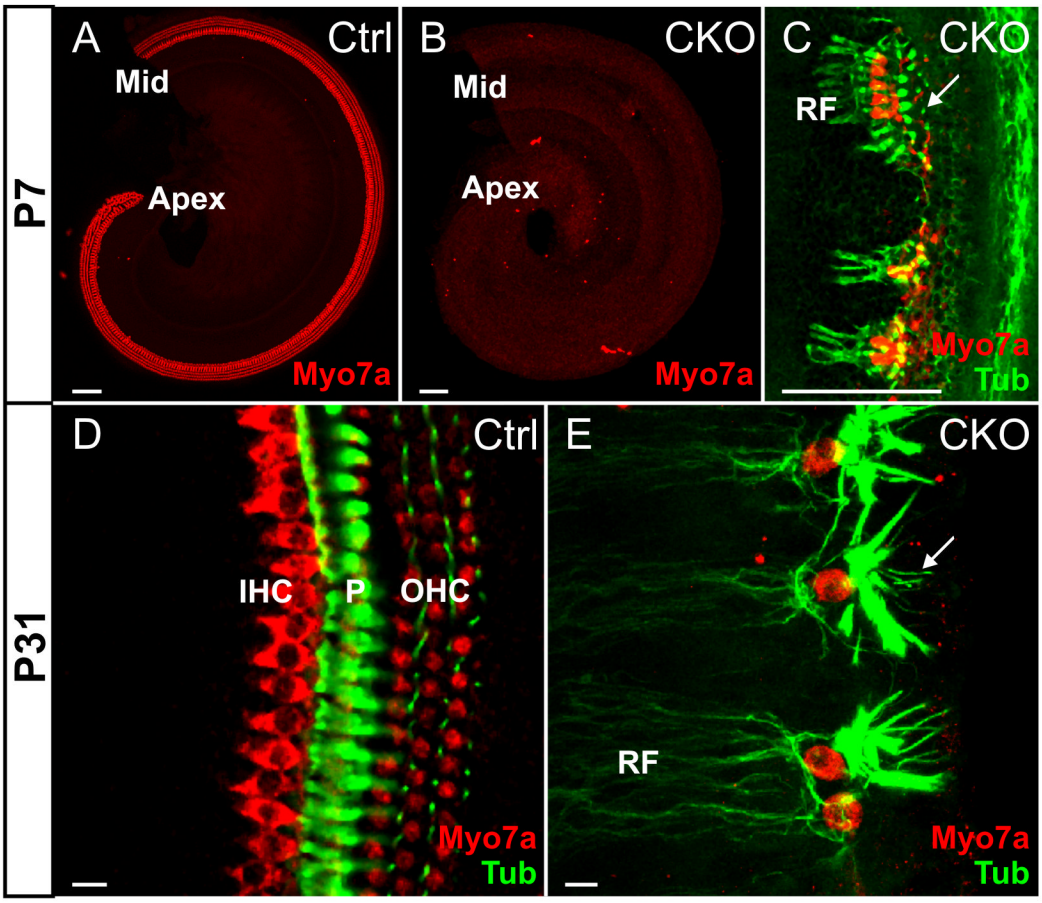


**Figure 7. Some Myo7a positive cells develop later in postnatal CKO mice**

Consistent with the absence of *Atoh1 in situ* signal in the *Atoh1* CKO mice, no Myo7a immunopositive cells are found in the mutant embryos, newborns, or in most postnatal mice up to P7 (B). However in some CKO cochlea, especially in late stages, there are few Myo7a positive cells detected (C, E). These few Myo7a positive cells are seen either individually or in small clusters. They receive the majority of the remaining nerve fibers and are more laterally flanked by Tubulin positive cells shaped either like pillar cells or Deiter's cells with thin phalangeal processes (arrows in C and E). IHC, inner hair cell; Mid, the middle part of the cochlea; OHC, outer hair cell; P, pillar cells; RF, radial fibers. Bar indicates 100 μm in A–C and 10 μm in D and E.

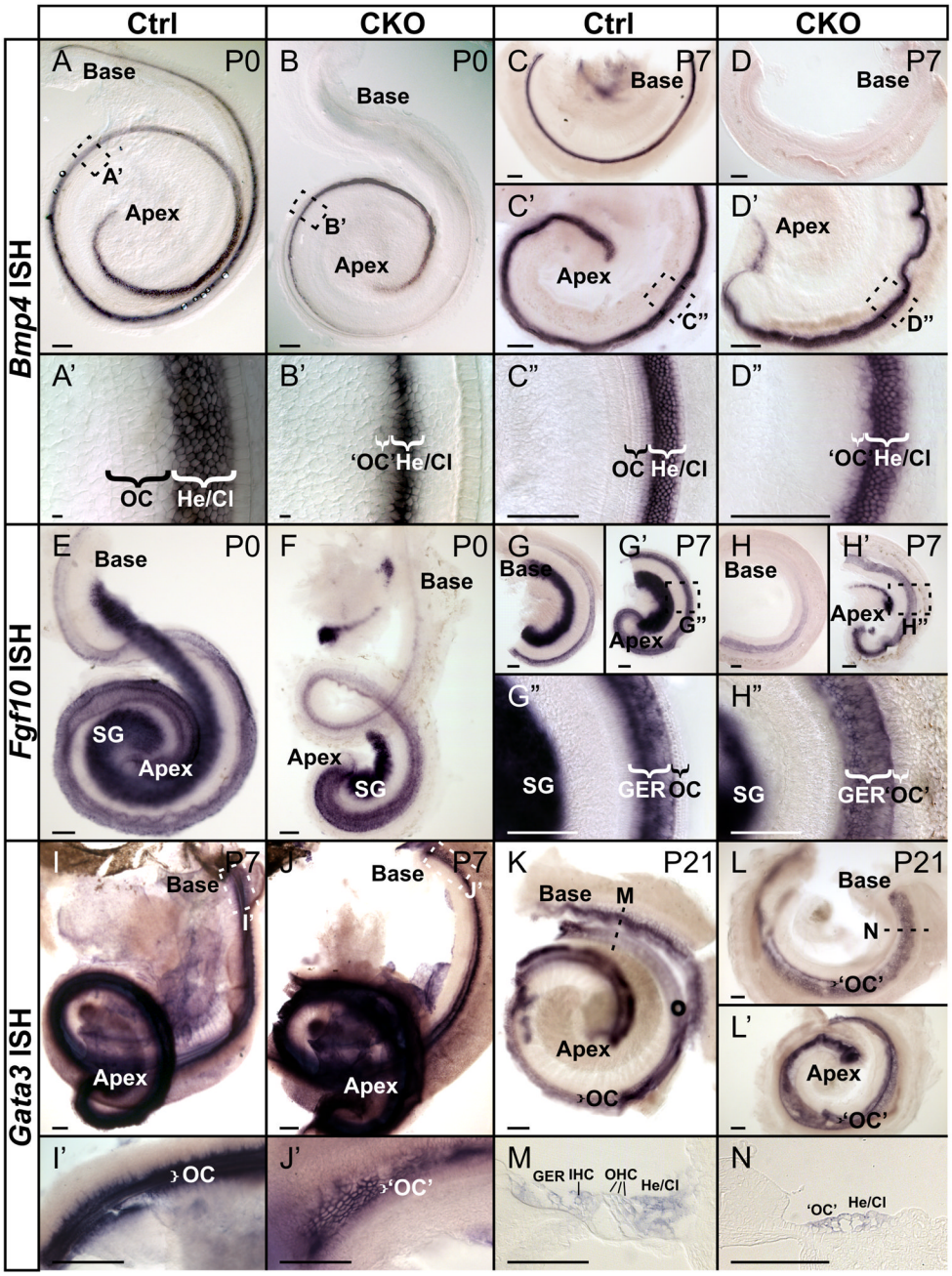


**Figure 8. Expression of several genes defines the undifferentiated organ of Corti in *Atoh1* CKO mutant**

(**A–D″**) *Bmp4* defines the lateral boundary of the organ of Corti and is retained in the apex of the mutant cochlea. *Bmp4 in situ* hybridization shows an apex to base gradient in Hensen's and Claudius cells lateral to the hair cells of the organ of Corti in P0 and P7 control mice (A, A′, C–C″). Likewise, *Atoh1* CKO mice display a gradient of *Bmp4* expression that is almost restricted to the apical half (B, B′, D–D″) and progressively lost in the base of the cochlea from P0 to P7 (B, D). Note the wider *Bmp4* expression area in D″ is more closer to the apex than the area in B', both of which appear to be restricted to the Hensen's cells and Claudius cells in the absence of differentiation of the organ of Corti (B′, D″). (**E–H″**) *Fgf10* defines the medial boundary of the organ of Corti. *Fgf10* is expressed in

the greater epithelial ridge (GER) in both control animals (E, G–G″) and also in CKO mice medial to the undifferentiated organ of Corti (F, H–H″). Like *Bmp4*, *Fgf10* is also downregulated in the basal half of cochlea in the absence of *Atoh1* compared to control littermate. (**I–N**) *Gata3* is expressed in the organ of Corti in P7 and P21 control mice and shows a similar expression pattern in the area of the putative organ of Corti in *Atoh1* CKO mice. Higher magnifications and sections reveal the distribution of *Gata3 in situ* reaction product in the organ of Corti and adjacent cells in control mice (I′, M). In *Atoh1* CKO mice, *Gata3* is expressed in undifferentiated cells that are topographically equal to the organ of Corti cells (J′, N). Cl, Claudius cells; GER, greater epithelial ridge; He, Hensen's cells; IHC, inner hair cell; OC, organ of Corti; 'OC', putative organ of Corti in *Atoh1* CKO; OHC, outer hair cell; SG, spiral ganglion. Bar indicates 100 μm in all except in A′, B′, M, N where it indicates 10 μm.

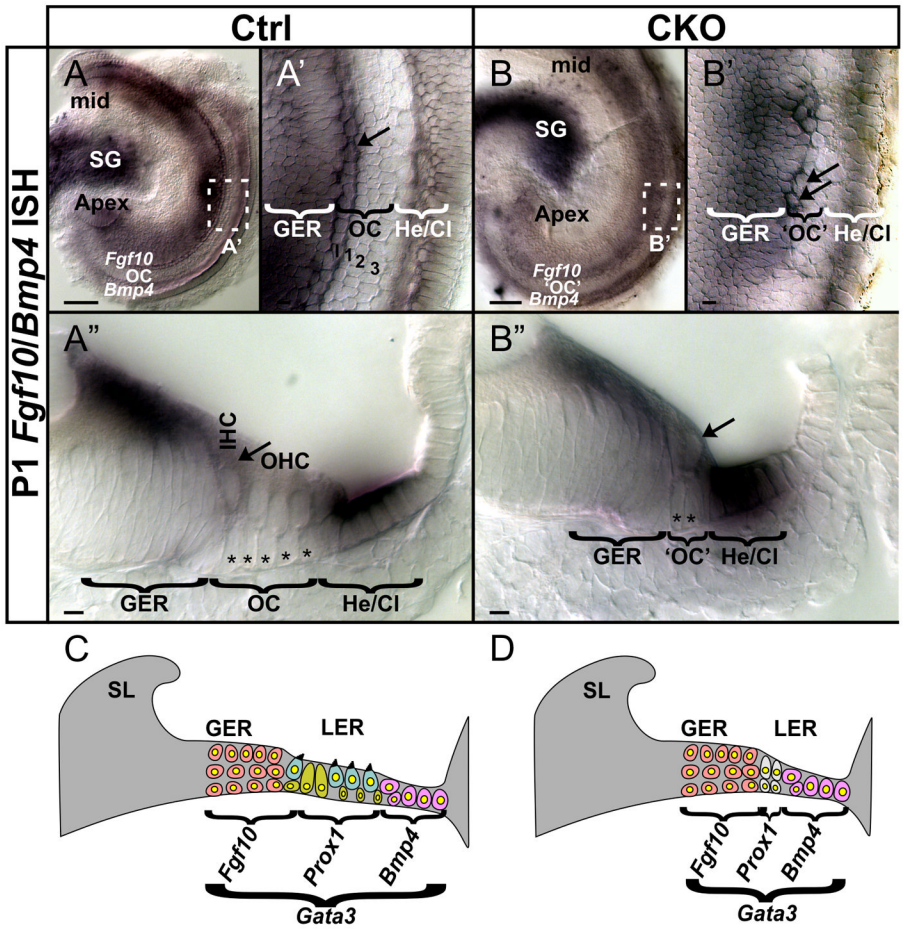


**Figure 9. Flanking markers define the cellular loss of the organ of Corti in the *Atoh1* CKO mutant**

(**A**–**B**″) *Fgf10* and *Bmp4* expression shown by double *in situ* hybridization defines the region between the two expression domains to be the organ of Corti. The P1 control mice have differentiated supporting and hair cells in this region (A, A′, with I, 1, 2, 3 in A′ indicating the inner and three rows of outer hair cells respectively), whereas only two rows of undifferentiated cells remain in the *Atoh1* CKO mice (B, B′). Radial sections show the degree of differentiation of hair cells and supporting cells (stars in A″) in the control cochlea between the two areas of marker expression (*Fgf10* medially and *Bmp4* laterally). At this stage, *Fgf10* also appears to be expressed in the inner hair cells (arrow in A″). However in the mutant cochlea, the two areas of marker expression are only separated by two rows of cells of the putative organ of Corti (B″), with patchy cells at the position of inner hair cells also expressing *Fgf10* (arrows in B′ and B″). (**C, D**) Schematic diagrams summarize the cellular loss of organ of Corti and the marker gene expression pattern change in the *Atoh1* CKO mutant. Cl, Claudius cells; GER, greater epithelial ridge; He, Hensen's cells; IHC, inner hair cell; LER, lesser epithelial ridge; Mid, the middle part of the cochlea; OC, organ of Corti; 'OC', putative organ of Corti in *Atoh1* CKO; OHC, outer hair cells; SG, spiral ganglion; SL, spiral limbus. Bar indicates 100 μm in A, B and 10 μm in A′, A″, B′, B″.

## Table 1

*Atoh1* CKO mice had near normal cochlear extension, but had no recognizable organ of Corti, narrowed basilar membrane and greatly reduced spiral ganglion.

| | Control | *Atoh1* CKO | % of reduction |
|---|---|---|---|
| **Length of cochlea (μm)**[a] | 5338±341[b] | 5045±374[c] | 5.5 |
| **Number of efferent fibers** | 475[d] | 44 | 91 |
| **Number of nerve fibers in the cochlea nerve** | ~10000[e] | 547 | 95 |
| **Length of basilar membrane (μm)** | 6436 | 5861 | 8.9 |
| **Average width of basilar membrane (μm)** | 127.6 | 58.65 | 54 |
| **Volume of basilar membrane (nL)** | 9.980 | 4.488 | 55 |
| **Volume of organ of Corti (nL)** | 12.99 | 0[f] | 100 |
| **Volume of Rosenthal's canal (nL)** | 52.35 | 5.197 | 90 |
| **Volume of tectorial membrane (nL)** | 14.0 | 6.172 | 56 |
| **Volume of scala media (nL)** | 274.5 | 229.8 | 16 |
| **Volume of scala vestibuli (nL)** | 478.1 | 450.5 | 5.8 |
| **Volume of scala tympani (nL)** | 485.2 | 465.4 | 4.1 |

[a], cochlea length was measured in whole mount preparation;

[b], n=3, shown here is average length±S.D;

[c], n=3, shown here is average length±S.D;

[d], (Campbell et al., 1988);

[e], (Anniko et al., 1988);

[f], no recognizable organ of Corti was found in *Atoh1* CKO mutant ear